Bioorganic Chemistry 111 (2021) 104973

Contents lists available at ScienceDirect

Bioorganic Chemistry

journal homepage: www.elsevier.com/locate/bioorg

Design, synthesis and *in vivo* anticancer activity of novel parthenolide and micheliolide derivatives as NF-κB and STAT3 inhibitors

Binglin Zeng [1], Yu Cheng [1], Kailu Zheng, Shuoxiao Liu, Longying Shen, Jinping Hu, Yan Li [*], Xiandao Pan [*]

State Key Laboratory of Bioactive Substance and Function of Natural Medicines and Beijing Key Laboratory of Active Substances Discovery and Druggability Evaluation, Institute of Materia Medica, Chinese Academy of Medical Sciences and Peking Union Medical College, Beijing 100050, PR China

ARTICLE INFO

Keywords:
Parthenolide
Micheliolide
Glioblastoma
Anticancer
STAT3

ABSTRACT

Parthenolide and micheliolide have attracted great attention in anticancer research due to their unique activities. In this study, thirteen parthenolide derivatives and twenty-three micheliolide derivatives were synthesized. Most synthesized compounds showed higher cytotoxicity than parthenolide or micheliolide. The *in vivo* anticancer activity of several representative compounds was evaluated in mice. One micheliolide derivative, 9-oxomicheliolide (**43**), showed promising *in vivo* antitumor activity compared with clinical drugs cyclophosphamide or temozolomide. Compound **43** was particularly effective against glioblastoma, with its tumor inhibition rate in mice comparable to the drug temozolomide. The discovery of compound **43** also demonstrates the feasibility of developing anticancer micheliolide derivatives by modification at C-9 position. Anticancer mechanism studies revealed that 9-oxomicheliolide exhibited inhibition effect against NF-κB and STAT3 signaling pathways, as well as induction effects of cell apoptosis. It is postulated that 9-oxomicheliolide is likely to be a modulator of the immune system, which regulates the anticancer immune responses.

1. Introduction

Parthenolide (PTL, **1**, shown in Fig. 1), a naturally occurring sesquiterpene lactone derived from medicinal plants, has attracted numerous attentions in recent years owing to its unique anticancer activity. Studies have found that PTL, independently or cotreated with other drugs, showed a broad spectrum of cancer inhibition, including leukemia, lymphoma, bone cancer, and breast cancer [1–4]. Its anticancer efficacy could be attributed to its strong inhibition against nuclear factor kappa B (NF-κB) and the pro-apoptotic effect by increasing reactive oxygen species (ROS) production [5]. Dimethylaminoparthenolide (DMAPT, **2**), a PTL derivative which is 1000 times more soluble than PTL, is subjected to clinical trials for the treatment of acute myeloid leukemia. However, although many efforts have been devoted to the bioactivity research of PTL, PTL still faces challenges limiting its clinical applications, including ineffectiveness toward bulk tumor cells *in vivo* or low metabolic stability [1,2], encouraging extensive research on PTL derivatization [2].

Recently, micheliolide (MCL, **3**), another sesquiterpene lactone which could be produced from parthenolide [6], has shown great potential in cancer treatment. MCL has been reported to inhibit NF-κB signaling pathway [7,8] and STAT3 (signal transducer and activator of transcription 3) signaling pathway [9], activate pyruvate kinase M2 (PKM2) [10], and decrease lipopolysaccharide-induced responses [11]. Due to its promising anticancer activity, ACT001 (**4**), fumarate salt form of dimethylaminomicheliolide as an orally available derivative of MCL, is currently under clinical trials in several countries for the treatment of glioblastoma [12]. Glioblastoma is an extremely aggressive and serious type of brain tumor with poor prognoses, and it is reported that in USA the median survival time for all patient diagnosed with glioblastoma in 2005–2008 was only 9.7 months [13]. The efficacy of ACT001 toward glioblastoma demonstrates the great potential of MCL in cancer treatment, and appropriate MCL derivatization may further enhance its biological activity [14,15]. However, one obstacle for MCL derivatization is its limited number of modification sites. Previous structure–activity relationship study has pointed out the importance of the 1,10-double bond [16] and α-methylene-γ-lactone [17], as modifications of either site usually led to decreased anticancer activity. Therefore, it

* Corresponding authors.
E-mail addresses: liyanxiao@imm.ac.cn (Y. Li), xdp@imm.ac.cn (X. Pan).
[1] B. Zeng and Y. Cheng contributed equally.

https://doi.org/10.1016/j.bioorg.2021.104973
Received 2 February 2021; Received in revised form 26 April 2021; Accepted 5 May 2021
Available online 15 May 2021

would be necessary and meaningful to develop new modification sites outside these known crucial regions which are responsible for the anticancer activity. In this respect, C-9 position of MCL, which could be derivatized via allylic oxidation, becomes a favorable site for modification to exert the full potential of MCL without harming the integrity of these biologically active moieties.

The esterification of PTL or MCL with carboxylic acid has been demonstrated to be an effective approach to improve anticancer activity of PTL or MCL [18–20]. Our previous study has shown that the conjugation with certain carboxylic acids could increase the anticancer activity and improve their pharmacological properties [21]. In addition, functional groups with strong antitumor activity (such as 1,8-naphthalimide or anthracycline) could also be coupled with PTL or MCL to exert synergistic effects. In this research, we report a new series of MCL derivatives with carboxylic ester groups at C-9 position of MCL. Twenty-three novel MCL derivatives of this type were synthesized and their structure were characterized. Thirteen novel PTL derivatives were also synthesized. Their *in vitro* and *in vivo* inhibiting activities toward multiple mice tumor models were evaluated. The preliminary anticancer mechanisms of the most active compounds were also studied and discussed.

2. Results and discussion

2.1. Chemistry

The synthesis procedures of PTL and MCL derivatives are shown in Scheme 1. PTL (**1**) was first oxidized with SeO_2/*t*-BuOOH to give melampomagnolide B (MMB, **5**) in 47% yield. MMB (**5**) was then coupled with various organic acids in the presence of 1-ethyl-3-(3-dimethylaminopropyl) carbodiimide hydrochloride (EDCI) to yield a series of esters **6**–**18** in yields of 16–79%. PTL (**1**) was also rearranged into MCL (**3**) in 82% yield catalyzed by *p*-toluenesulfonic acid [6]. MCL (**3**) was then oxidized with SeO_2/*t*-BuOOH to give derivatives **19**, **20**, and **21**, in yields of 53%, 14%, and 7%, respectively. The hydroxy group at C-9 position of compound **19** was determined to be in *S* configuration by 2D ^{1}H–^{1}H nuclear overhauser effect spectroscopy (NOESY). The NOESY cross-peaks between H-9 and H-7 revealed that these two H atoms oriented the same side of the ring system, which indicated compound **19** was a single stereoisomer (shown in Fig. S84 in Supplementary Information). Compound **19** was then reacted with various acids to yield MCL esters **23**–**42** (yield: 33–68%) in the presence of EDCI. Compound **19** could also be directly oxidized by Dess-Martin periodinane to produce 9-oxomicheliolide **43** in the yield of 80%.

Compound **21** was obtained from the allylic oxidation of MCL. The structural elucidation of compound **21** was accomplished by high resolution mass spectroscopy (HRMS), ^{1}H and ^{13}C 1D nuclear magnetic resonance (NMR), and multiple 2D NMR techniques, including NOESY, heteronuclear single quantum correlation (HSQC), and heteronuclear multiple bond correlation (HMBC). Spectrums were presented in the Supplementary Information. The molecular formula of compound **21** was determined as $C_{15}H_{20}O_4$ by HRMS, suggesting that it was an isomer of compound **19**. The ^{1}H NMR spectrum of compound **21** indicated one more olefinic hydrogen [δ_H 5.85–5.87 (m, 1H, H-2)] than compound **19**. ^{13}C NMR suggested that the hydroxymethyl unit in compound **19** was replaced by an oxygen-bearing quaternary carbon (δ_C 70.9) in compound **21**, implying the transposition of the tetrasubstituted double bond and the hydroxy group. In the HMBC spectrum of compound **21**, correlations from H-5 (δ_H 3.06) to C-1 and C-2, from H-14 (δ_H 1.49) to C-1, C-10 and C-9, and from H-15 (δ_H 1.40) to C-3, C-4 and C-5, together with their chemical shifts, positioned the double bond between C-1 and C-2 and the two hydroxyls at C-4 and C-10. In the NOE difference spectrum of compound **21**, irradiation of H-14 enhanced H-2 and H-7, while H-7 and H-3a were enhanced by irradiation of H-5. These enhancements indicated that H-3a, H-5, H-7, and H-14 were oriented on the same side of the ring system. In addition, H-6 and H-3b were enhanced by irradiation of H-15, indicating that these hydrogen atoms were oriented on the other side. Therefore, the structure of compound **21** was confirmed as shown, and major correlations were indicated in Fig. 2.

During the synthesis of compound **43**, compound **44** was also discovered by accident. The synthesis of compound **43** was performed using crude **19** produced by the oxidation of compound **3** without purification. Unexpectedly, during the purification of compound **43**, an unknown compound **44** was obtained in 13% yield. The molecular formula of compound **44** was determined as $C_{15}H_{18}O_4$ by HRMS, indicating compound **44** to be an isomer of compound **43**. In order to confirm the structure of compound **44**, multiple 2D NMR experiments were conducted, and spectrums could be found in Supplementary Information. Comparison of ^{13}C NMR spectrums between compound **19** and **44** implied that a hydroxymethyl carbon from the former was replaced by a carbonyl carbon in the latter. HSQC and COSY (2D ^{1}H–^{1}H correlated spectroscopy) analysis revealed the presence of vicinal coupling fragment of H-5/H-6/H-7/H-8/H-9 as well as two isolated units H-3 and H-13 as shown in Fig. 2. The HMBC spectrum of compound **44** suggested the long-range heteronuclear correlations from H-3 to C-1, C-2, C-4 and C-5, and from H-15 to C-3, C-4 and C-5. These correlations, together with the chemical shift of the correlated proton and carbon resonances, suggested compound **44** was a 2-one derivative of MCL (**3**). This supposition was further verified using HMBC by the correlation from H-6 to C-12, from H-13 to C-7, C-11 and C-12, and from H-14 to C-1, C-9, and C-10, as well as their chemical shifts. In the NOESY spectrum of compound **44**, the NOE cross-peaks between H-5 and H-7 and between H-6 and H-15 indicated that the configuration of compound **44** retained the same chirality as that of MCL. Based on these careful structural characterizations, the structure of compound **44** was determined as shown in Scheme 1. It is speculated that compound **44** was produced by the oxidation of a presumed compound **22**. However, we were unable to obtained purified compound **22** for structure characterization, so brackets were used to denote compound **22** in Scheme 1 as a presumed compound. Although the structure of compound **44** has been reported in a previous patent via chemoenzymatic methods [15], this work is first to report the chemical synthesis of compound **44**.

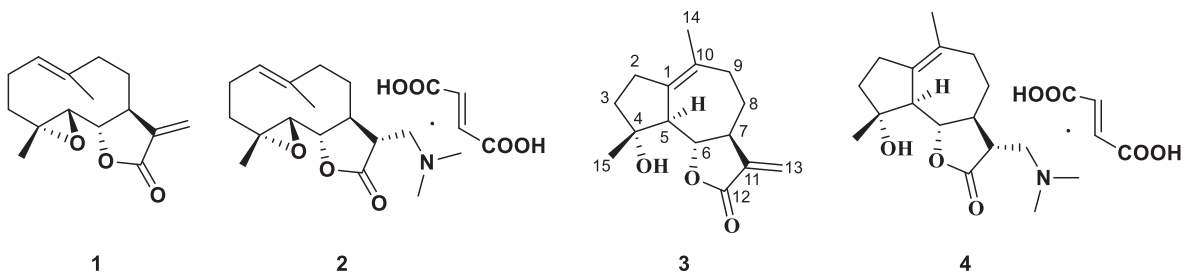

Fig. 1. The structure of PTL (**1**), DMAPT (**2**), MCL (**3**), and ACT001 (**4**).

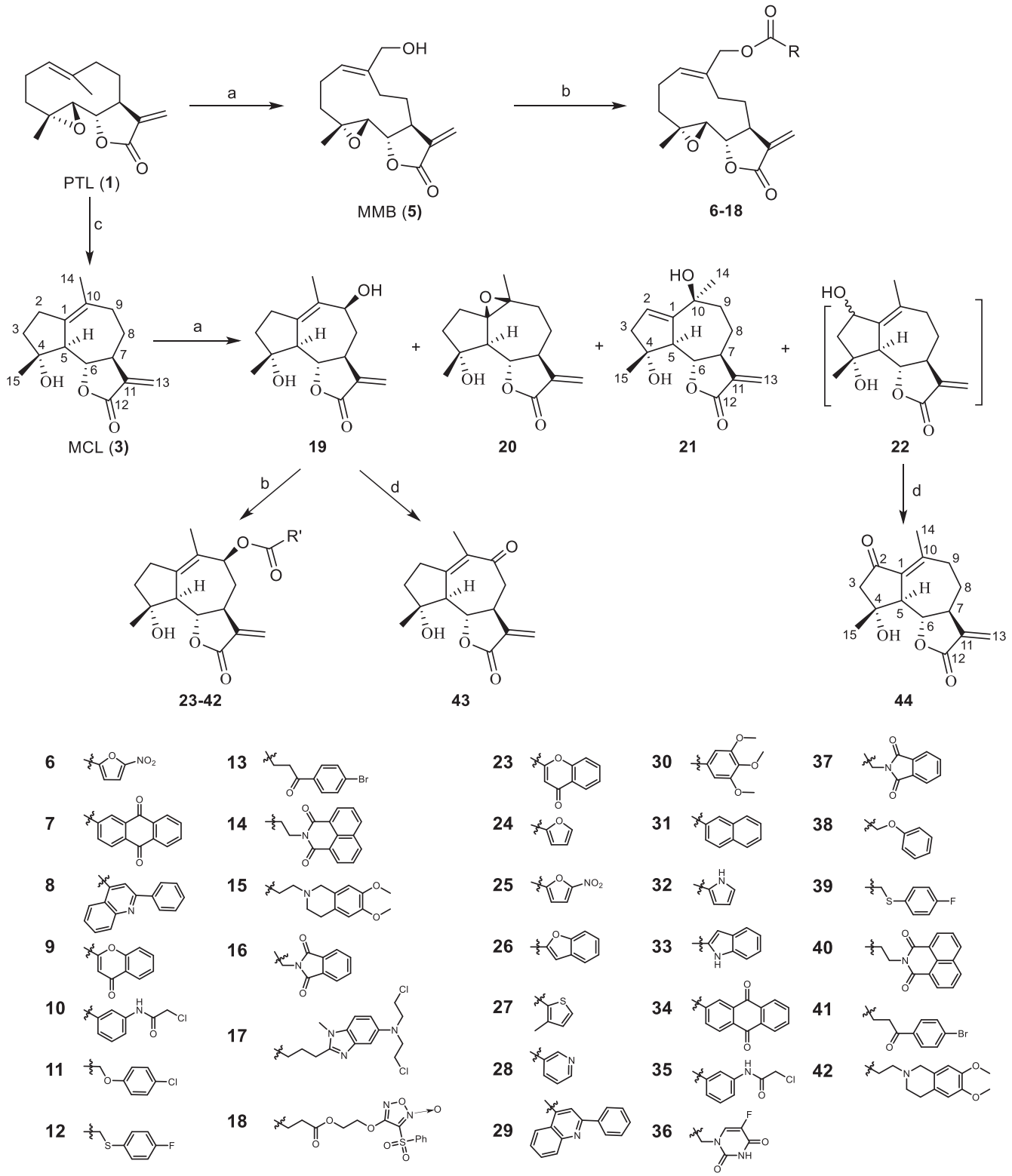

Scheme 1. General synthesis of MCL derivatives (**8**–**44**). Reagents and conditions: (a) SeO_2/*t*-BuOOH, RT, 3 h; (b) EDCI, DMAP, carboxylic acid, CH_2Cl_2, RT, 3 h; (c) PTSA, CH_2Cl_2, RT, overnight; (d) Dess-Martin periodinane, $NaHCO_3$, CH_2Cl_2, RT, 3 h.

2.2. In vitro cytotoxic studies

The *in vitro* antiproliferative activity of synthesized compounds was evaluated in five human cancer cell lines using the MTT assay, including HCT116 (colorectal carcinoma), U87MG (glioblastoma), HepG2 (hepatocellular carcinoma), BGC823 (gastric carcinoma), and PC9 (lung adenocarcinoma). Paclitaxel (PTX) was used as the experiment control. PTL and MCL were used as positive controls due to their NF-κB and STAT3 inhibition effect [5,22,23]. MMB has been demonstrated to show anticancer activity comparable to PTL [24], so MMB was also included for comparison. The results are shown in Table 1. It could be seen in the table that all synthesized compounds showed moderate to significant

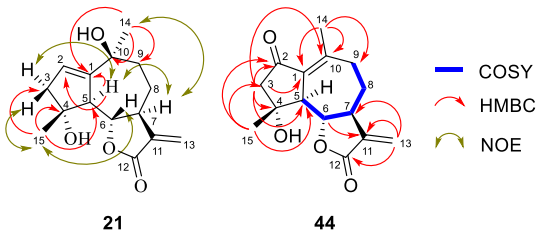

Fig. 2. Key COSY, HMBC and NOE correlations of compound **21** and **44**.

Table 1
In vitro antitumor activity of synthesized compounds in five human cancer cell lines.

Compd	IC_{50} (μmol/L)				
	HCT116	U87MG	HepG2	BGC823	PC9
1 (PTL)	18.31	8.40	8.93	19.49	26.44
3 (MCL)	37.11	12.85	17.58	21.05	27.47
5 (MMB)	4.16	6.08	15.78	9.23	7.99
6	4.60	4.14	3.45	7.27	3.82
7	16.76	16.58	9.57	12.23	9.68
8	2.11	2.47	4.71	5.23	3.00
9	18.94	19.95	16.91	19.45	17.10
10	2.11	5.98	1.46	1.93	2.85
11	16.47	16.42	15.06	6.66	7.50
12	16.75	16.20	14.06	16.92	14.98
13	7.82	7.83	9.27	6.99	9.80
14	2.55	3.91	2.90	2.87	4.67
15	3.90	4.73	3.20	1.91	7.20
16	2.15	1.58	1.02	1.29	13.87
17	15.12	7.96	13.22	7.48	5.65
18	12.38	0.11	0.41	1.81	4.56
19	36.75	37.19	19.19	21.15	37.91
23	20.87	0.21	10.28	20.94	28.34
24	21.67	17.59	7.02	15.02	28.46
25	20.91	28.77	15.82	18.38	27.03
26	19.07	6.99	8.66	11.45	16.06
27	6.29	4.49	3.67	7.60	6.44
28	13.58	13.44	9.82	10.52	24.29
29	21.01	7.42	9.92	15.74	13.74
30	13.56	15.29	8.94	24.58	14.61
31	4.10	2.78	2.95	5.22	5.91
32	18.16	29.23	29.40	33.79	42.77
33	10.87	7.07	12.17	18.23	17.97
34	5.73	5.50	4.60	3.71	6.55
35	4.32	3.90	4.15	6.43	5.61
36	44.13	29.10	23.91	27.81	33.07
37	21.97	28.26	14.33	16.64	27.05
38	>50.00	>50.00	26.41	44.26	>50.00
39	4.49	11.63	10.05	31.08	15.05
40	5.47	3.18	4.03	11.00	5.14
41	7.87	6.25	5.80	15.44	8.50
42	16.61	23.32	14.96	>50.00	32.38
43	38.09	13.15	16.60	14.27	40.04
PTX	0.000389	0.006757	0.007143	0.001098	0.000603

potency toward five cancer cell lines. It could be noticed that the cytotoxicity of most PTL and MCL esters was higher than that of PTL or MMB, respectively, indicating that esterification could improve the *in vitro* anticancer activity. Several PTL derivatives, including esters **8**, **10**, **14**, and **15**, exhibited higher cytotoxicity against all five cell lines than PTL and MMB. It is worth noting that compounds **16** and **18** showed IC_{50} values of 1.58 μM and 0.11 μM against glioblastoma U87MG, respectively. These results suggested that the heterocyclic carboxylic acid conjugates could effectively increase the anticancer potency of PTL.

For MCL esters, most compounds showed higher cytotoxicity than MCL, with several compounds, such as compounds **27**, **31**, **34**, and **35,** showing strong potency. This indicated that the structure modification of MCL by adding ester moieties at C-9 position could further increase its biological activity. Moreover, because the hydroxy group at C-9 position could be readily converted into various linker groups, MCL molecule could form conjugates with numerous compounds via C-9 position without sabotaging the biological activity of MCL. This introduction of hydroxy group at C-9 position will provide plentiful opportunities for designing novel MCL derivatives and studying the structure–activity relationship in the future.

2.3. *In vivo* anticancer activity

Based on the cytotoxicity results, it is necessary to further evaluate the *in vivo* antitumor activity of synthesized compounds. The metabolic stability of PTL derivatives was reported before [25], while relevant studies on MCL derivatives were scarce. In some cases, carboxylic esters are subjected to fast hydrolysis *in vivo*. In order to demonstrate whether esters synthesized in this study are metabolically stable *in vivo*, a preliminary pharmacokinetic study on a representative MCL ester **31** in mice after a single oral administration at 100 mg/kg was conducted. As shown in Fig. 3, the plasma concentration of ester **31** remained relatively stable from 0.5 to 8 h, indicating that carboxylic esters synthesized in this study were likely to be stable in the body several hours after oral administration.

Several PTL and MCL derivatives were selected for *in vivo* anticancer activity evaluation in tumor-bearing mice. PTL esters **16** and **18** with high cytotoxicity toward glioblastoma were tested against H22 murine hepatocellular carcinoma and C26 murine colon carcinoma at two different doses, and the results were shown in Tables S1 and S2 of the Supplementary Information, respectively. To our surprises, although promising *in vitro* activity was shown for both compounds, esters **16** and **18** showed low *in vivo* activity at both doses. Low inhibition activity was observed against H22 tumor, while no tumor inhibition activity was observed against C26 tumor. Although parthenolide and its orally available form DMAPT hold high promises as candidates for anticancer drugs recently, two of its ester derivatives synthesized in this study showed low *in vivo* antiproliferative activity.

Four MCL derivatives (compounds **25**, **30**, **31** and **43)** were also evaluated in H22 and G422 mouse tumor models. Esters **25** and **30** were chosen for *in vivo* tests due to their substitutional groups which have been proven to be highly active against cancer [20,26]. Compound **31** was chosen due to its high cytotoxicity as shown in Table 1. Compound **43**, namely 9-oxomicheliolide, was tested to reveal the effect of the carbonyl group at C-9 position. Cyclophosphamide (CTX) or temozolomide (TMZ) were used as positive control. Compound **25** was only evaluated in H22 model. The results are shown in Tables 2 and 3. In contrast with PTL esters, all four MCL derivatives turned out to be relatively effective in eradicating tumor cells in mice than PTL esters. Compounds **31** and **43** showed the inhibitory rate of 51.70% and

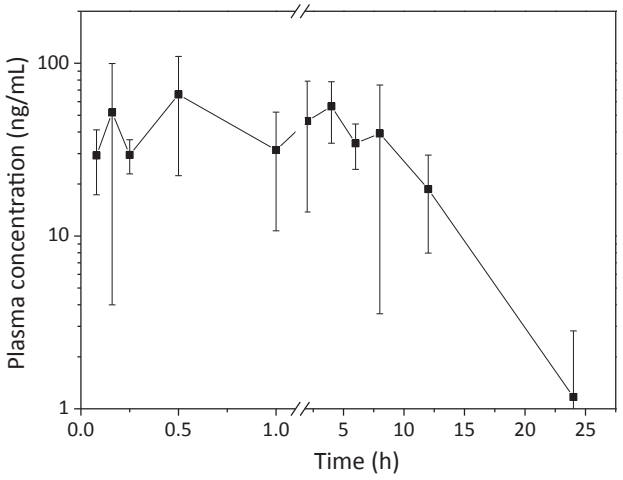

Fig. 3. Pharmacokinetic study of compound **31** in mice after a single oral administration at 100 mg/kg.

Table 2
In vivo anticancer activity of MCL derivatives against H22-bearing mice (mean ± SD).[a]

Group	Dose (mg/kg)	Schedule	Body weight (g)		Tumor weight (g)	Inhibition rate (%)
			Beginning	End		
Control			16.9 ± 1.0	28.1 ± 1.9	3.53 ± 0.39	
CTX	60.0	1	16.3 ± 0.6	26.6 ± 3.0	1.41 ± 0.65***	60.01
25	100.0	1–9	16.3 ± 0.5	27.6 ± 1.8	1.90 ± 0.63***	46.27
30	100.0	1–9	16.4 ± 0.3	27.1 ± 3.3	2.04 ± 0.50***	42.16
31	100.0	1–9	16.4 ± 0.6	27.1 ± 1.1	1.71 ± 0.45***	51.70
43	100.0	1–9	16.6 ± 0.4	24.8 ± 5.2	1.58 ± 0.34***	55.29

[a] Eight mice were in each experiment group. Significant values are *** $P < 0.001$.

Table 3
In vivo anticancer activity of MCL derivatives against G422-bearing mice (mean ± SD).[a]

Group	Dose (mg/kg)	Schedule	Body weight (g)		Tumor weight (g)	Inhibition rate (%)
			Beginning	End		
Control			19.5 ± 0.8	35.7 ± 2.6	4.10 ± 1.17	
TMZ	30.0	1–5	19.2 ± 0.3	34.9 ± 2.4	0.76 ± 0.49***	81.40
30	200.0	1–13	19.3 ± 1.0	35.2 ± 3.1	2.91 ± 1.28	28.96
31	200.0	1–13	20.3 ± 1.1	35.6 ± 3.5	2.95 ± 1.59	27.93
43	100.0	4–8,10,12	19.2 ± 1.0	36.3 ± 0.9	1.65 ± 1.02*	59.78

[a] Five mice were in each experiment group. Significant values are *$P < 0.05$, and ***$P < 0.001$.

55.29%, respectively, toward H22 tumor cells. Based on this research, it could be concluded from both *in vitro* and *in vivo* results in this work that the MCL derivatization at C-9 position is an effective, and also a promising approach to develop MCL derivatives with higher anticancer efficacy.

Notably, compound **43**, which showed moderate *in vitro* cytotoxicity, was remarkably effective toward both tumors in mice. The anticancer activity of compound **43** was effective against H22 tumor cells, and it also showed considerable inhibition effect toward G422 glioblastoma. Glioblastoma is an aggressive type of brain cancer with few therapeutic approaches, and temozolomide is currently the most widely used chemotherapy drug for glioblastoma. Interestingly, the distinct performance of compound **43** from *in vitro* and *in vivo* experiments implies that compound **43** is more likely to be an agent that could regulate anticancer immune responses, rather than a cytotoxic drug directly resulting in cell death. This is inspired by the fact that ACT001 (**4**), an orphan drug currently in clinical trials for the treatment of glioblastoma, is also reported to possess immunomodulatory effects [12]. The preliminary result in this study demonstrates the high potential of compound **43** as a drug candidate especially targeting glioblastoma, and this was studied in detail in the following sections.

2.4. Effects of 43 doses in H22- and G422-bearing mice

Encouraged by the preliminary result of compound **43** in suppressing H22 and G422 tumor proliferation in Tables 2 and 3, more *in vivo* experiments were conducted to further investigate the anticancer effect of compound **43** against both murine tumor models. Mice bearing H22 tumors were treated with different doses of compound **43**, and results are shown in Table 4, along with the image of excised tumors from mice after treatment in Fig. 4. 5-Fluorouracil (5-FU) was used as the positive control. All mice survived to the end of the treatment. With the dose increasing from 10 to 30 mg/kg, the inhibition effect of compound **43** against H22 tumor increased, approaching the inhibition rate of 5-FU at 30 mg/kg. The images of excised tumors indicated the similar conclusion, as mice treated with 30 mg/kg of compound **43** resulted in tumor size similar to those treated with 5-FU. These results again demonstrated the remarkable anticancer activity of compound **43** even comparing to the chemotherapy drug 5-FU.

In order to study the effect of tested compounds on the immune system, spleen index and thymus index, measures of the volume of spleen and thymus, respectively, were also presented in Table 4. It could be seen that spleen index and thymus index in the 5-FU-treated group decreased drastically compared with the control group, which is consistent with a previous study [27]. Such a decrease indicated the strong suppression effect of 5-FU toward the immune system [28]. In contrast, mice treated with compound **43** showed similar spleen index and an increased thymus index compared with the control group, suggesting that compound **43** exerted little or no side effect on immune system, even though their tumor inhibition effect was similar.

For doses ranging from 10 to 30 mg/kg, the anticancer efficacy of compound **43** improved with increasing doses as shown in Table 4. Next, the doses were increased further up to 60 mg/kg, and the inhibitory effect of compound **43** in G422-bearing mice was studied. The results were shown in Table 5 and the excised tumors were shown in Fig. 5. Temozolomide (TMZ) was used as positive control. The inhibitory rate of compound **43** reached 69% when the dose was 40 mg/kg, only slightly lower than the inhibitory rate of temozolomide, the chemotherapy drug for glioblastoma. When the dose was increased from 40 to 60 mg/kg, the inhibitory rate decreased.

To investigate the cytotoxic effect of compound **43** on blood profile in animals, peripheral blood of mice from the tumor inhibition study described in Table 5 were collected and analyzed. The peripheral blood profiles were shown in Table 6. TMZ has been reported to result in myelotoxicity [29], and this is confirmed by this research as the red blood cell count (RBC) and platelet count (PLT) were both decreased from the control group. In contrary, mice treated with compound **43** showed blood profiles similar to the control group in most of the indices, demonstrating the relatively lower detrimental effect against blood system of compound **43** compared with TMZ. Also, every group of mice treated with compound **43** showed a marked increase in platelet count (PLT) compared with the control group. Previous research has proposed that parthenolide strengthen platelet formation owning to NF-κB inhibition [5,30]. Accordingly, it is deduced that compound **43** is likely to be a NF-κB inhibitor, similar to its structure analogue PTL and MCL.

2.5. The inhibitory effect of MCL derivatives on NF-κB and STAT3 signaling pathways

As MCL derivatives (especially **43**) showed encouraging *in vitro* and *in vivo* anticancer activity, it becomes imperative to reveal the probable mechanism of their anticancer activity. NF-κB and STAT3 signaling pathways have been proposed to play important and also complex roles in the proliferation, survival and apoptosis of many types of cancer, resulting in the suppression of the anticancer immune response [31–33]. Moreover, NF-κB and STAT3 are highly interconnected, as STAT3 could not only be activated by NF-κB expression but also contribute to the constitutive expression of NF-κB [34]. Previous study has identified MCL as an effective inhibitor of NF-κB pathway by inhibiting relevant kinases [7,8,12]. As for STAT3, although few studies have reported its inhibition by MCL derivatives, parthenolide and its derivatives have been confirmed to inhibit STAT3 pathway [9,35,36]. Based on these studies, it was speculated that the remarkable *in vivo* anticancer activity of MCL

Table 4
Effects of the doses of compound **43** in H22-bearing mice (mean ± SD).[a]

Group	Dose (mg/kg)	Schedule	Body weight (g)		Tumor weight (g)	Inhibition rate (%)	Spleen index (mg/10 g)[c]	Thymus index (mg/10 g)[d]
			Beginning	End				
Control			14.6 ± 0.3	25.4 ± 1.7	2.21 ± 0.65		114.61 ± 12.02	33.04 ± 4.04
5-FU	40.0	1,4,7	15.1 ± 0.4	22.7 ± 1.7**	0.73 ± 0.31***	67.12	57.01 ± 23.72***	8.59 ± 1.98***
43	10.0[b]	1–7	15.0 ± 0.6	26.5 ± 1.1	1.52 ± 0.33*	31.05	109.61 ± 21.43	45.09 ± 7.03**
	20.0	1–7	15.0 ± 0.5	27.7 ± 1.2**	1.40 ± 0.29**	36.45	107.37 ± 16.38	48.10 ± 4.65***
	30.0	1–7	14.8 ± 0.5	25.5 ± 1.5	0.76 ± 0.19***	65.42	98.79 ± 23.74	53.51 ± 9.18***

[a] Eight mice were in each group. Significant values are $*P < 0.05$, $**P < 0.01$, and $***P < 0.001$.
[b] Seven mice were in this group.
[c] Spleen index = spleen weight/(body weight × 10).
[d] Thymus index = thymus weight/(body weight × 10).

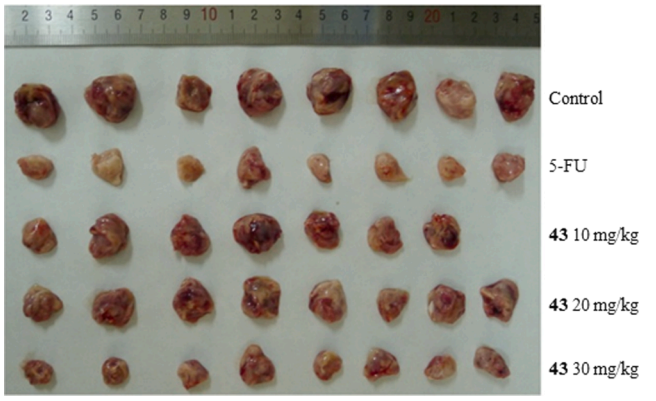

Fig. 4. Effect of compound **43** doses on H22-tumors excised from mice after treatments.

Fig. 5. Effect of compound **43** doses on G422-tumors excised from mice after treatments.

Table 5
Effects of the dose of compound **43** in G422-bearing mice (mean ± SD).[a]

Group	Dose (mg/kg)	Schedule	Body weight (g)		Tumor weight (g)	Inhibition rate (%)
			Beginning	End		
Control			16.5 ± 0.5	36.2 ± 2.4	2.30 ± 0.85	
TMZ	30.0	1–5	16.6 ± 0.6	32.9 ± 2.0	0.60 ± 0.29	73.98%***
43	10.0	1–13	16.3 ± 0.7	37.9 ± 2.4	2.11 ± 0.68	8.14%
	20.0	1–13	16.2 ± 0.8	36.7 ± 2.8	1.41 ± 0.42	38.70%*
	40.0	1–13	16.2 ± 0.4	34.1 ± 2.5	0.71 ± 0.48	69.25%**
	60.0	1–13	16.1 ± 0.6	34.7 ± 2.1	1.25 ± 0.66	45.47%*

[a] Seven mice were in each group. Significant values are $*P < 0.05$, $**P < 0.01$, and $***P < 0.001$.

derivatives (especially compound **43**) could also be ascribed to the suppression of NF-κB and STAT3 signaling pathways. To verify this hypothesis, the inhibitory effect of two MCL derivatives (compounds **23** and **43**) on the TNF-α-induced NF-κB signaling pathway and IL-6-induced STAT3 signaling pathway were evaluated using the luciferase reporter assay in HepG2 human liver carcinoma cell, and the results were shown in Fig. 6. For NF-κB signaling pathway, compound **23** showed a decreasing trend of the transcriptional activity with increasing concentration, while compound **43** showed a volcano-type relation with the maximum transcriptional activity appearing at around 1 μM. When the concentration increased from 10 to 100 μM, the NF-κB transcriptional activity were significantly reduced for both compound **23** and compound **43**. For STAT3 signaling pathway, a more explicit concentration-dependent relation was observed for both tested compounds, with the STAT3 transcriptional activity decreased with increasing concentration. From the experimental results in this study, it could be deduced that MCL derivatives could simultaneously suppress both NF-κB and STAT3 activation, relieving the immunosuppression effect exerted by NF-κB and STAT3, and promoting the antitumor immune response.

Previous studies indicated that α,β-unsaturated carbonyl groups, also known as Michael acceptors, play key roles in the inhibition of NF-κB or STAT3 signaling pathway [37,38]. α,β-unsaturated carbonyl groups could react with the sulfhydryl group of peripheral cysteine residues from proteins, resulting in an irreversible inhibition of the signaling pathway. Some sesquiterpene lactones showed inhibition toward NF-κB by alkylating cysteine residues of the p65 subunit of NF-κB through α,β-unsaturated carbonyl groups [39]. Similarly, galiellalactone and curcumin, which also possess α,β-unsaturated carbonyl moieties, have been shown to irreversibly modify the cysteine residues in the DNA binding domain of STAT3 and block its signaling [40,41]. In this respect, it is highly probable that the NF-κB and STAT3 inhibitory effect of MCL derivatives, especially compound **43**, is attributed to the α,β-unsaturated carbonyl structure. However, whether compound **23** or **43** targets other proteins in NF-κB and STAT3 signaling pathways is still unknown. The inhibition effect of compound **43** on inhibitor of NF-κB kinase-β (IKKβ), which is involved in the activation of NF-κB, was tested, and no signs of inhibition were observed (data not shown).

Based on the results in literature and in this work, a preliminary structure–activity relationship (SAR) using compound **43** as a model compound was proposed as shown in Fig. 7. Both α,β-unsaturated ketone (region A) and α-methylene-γ-lactone (region B) serve as crucial nucleophilic moieties to react with peripheral cysteine residues in a Michael-type addition and result in NF-κB or STAT3 inhibition. Region C and D was well tolerated to structure modifications and could act as sites for

Table 6
Peripheral blood profile of G422-bearing mice treated with **43** (mean ± SD).[a]

Index	Control	TMZ	**43** (10.0 mg/kg)	**43** (20.0 mg/kg)	**43** (40.0 mg/kg)	**43** (60.0 mg/kg)
WBC ($\times10^9$/L)	11.39 ± 1.96	10.54 ± 4.51	11.09 ± 2.75	10.16 ± 2.35	13.10 ± 3.27	11.77 ± 2.19
LYM (%)	11.07 ± 3.06	18.27 ± 9.56	10.74 ± 6.35	11.17 ± 5.03	7.41 ± 2.47*	9.10 ± 10.25
MON (%)	1.63 ± 1.16	3.33 ± 1.96	1.23 ± 1.13	1.40 ± 0.60	1.31 ± 1.14	1.06 ± 1.13
NEUT (%)	87.30 ± 4.02	78.40 ± 11.10	88.03 ± 7.26	87.43 ± 5.43	91.27 ± 3.30	89.84 ± 11.37
RBC ($\times10^{12}$/L)	6.80 ± 0.43	6.09 ± 0.35**	6.61 ± 0.84	6.66 ± 0.70	6.94 ± 0.36	6.46 ± 0.49
HGB (g/L)	94.00 ± 5.45	88.71 ± 5.31	90.00 ± 12.07	94.86 ± 10.22	96.43 ± 7.39	90.43 ± 7.04
HCT (L/L)	31.34 ± 1.93	29.33 ± 1.50	30.01 ± 3.46	31.13 ± 3.23	31.54 ± 1.91	29.81 ± 1.70
MCV (fl)	46.14 ± 1.80	48.23 ± 1.55*	45.49 ± 2.15	46.81 ± 2.06	45.46 ± 0.77	46.23 ± 2.01
MCH (pg)	13.84 ± 0.62	14.59 ± 0.41*	13.61 ± 0.93	14.26 ± 0.79	13.89 ± 0.51	14.00 ± 0.60
MCHC (g/L)	300.00 ± 4.47	302.43 ± 6.05	299.14 ± 8.88	304.57 ± 5.68	305.29 ± 7.16	303.00 ± 8.25
RDW (fl)	17.47 ± 1.34	17.07 ± 1.14	17.29 ± 1.23	16.99 ± 1.67	16.61 ± 1.45	16.37 ± 1.30
PLT ($\times10^9$/L)	603.71 ± 120.73	516.57 ± 146.28	687.71 ± 104.56	685.71 ± 112.70	746.14 ± 76.41*	707.14 ± 41.17
PCT (L/L)	0.34 ± 0.07	0.30 ± 0.08	0.39 ± 0.06	0.4 ± 0.06	0.43 ± 0.05*	0.40 ± 0.03*
MPV (fl)	5.56 ± 0.14	5.91 ± 0.25**	5.64 ± 0.16	5.76 ± 0.14*	5.70 ± 0.26	5.63 ± 0.26
PDW (fl)	12.89 ± 1.04	13.33 ± 0.50	12.90 ± 0.70	12.91 ± 0.69	12.74 ± 0.32	12.96 ± 0.64

[a] Significant values are *$P < 0.05$, **$P < 0.01$, and ***$P < 0.001$. Abbreviations: WBC, white blood cell count; LYM, lymphocytes; MON, mononuclear cells; NEU, neutrophils; RBC, red blood cell count; HGB, hemoglobin; HCT, hematocrit; MCV, mean corpuscular volume; MCH, mean corpuscular hemoglobin; MCHC, mean corpuscular hemoglobin concentration; RDW, red cell distribution width; PLT, platelet count; PCT, plateletcrit; MPV, mean platelet volume; PDW, platelet distribution width.

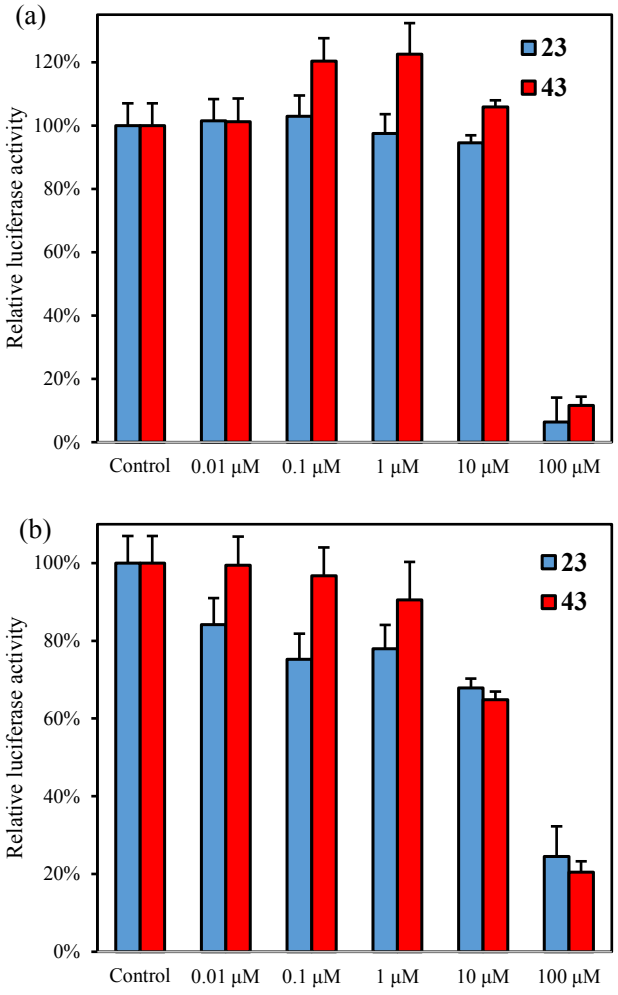

Fig. 6. The inhibition effect of different doses of compound **23** and **43** on (a) the TNF-α activated NF-κB-dependent transcriptional activity and (b) the IL-6 activated STAT3-dependent transcriptional activity using the luciferase reporter assay in HepG2 human liver carcinoma cells.

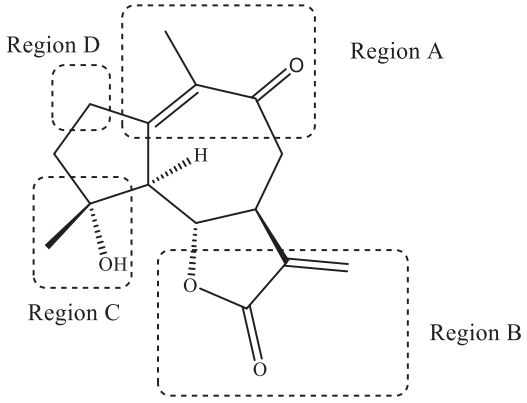

Fig. 7. The preliminary structure–activity relationship of compound **43**. Region A (*α,β*-unsaturated ketone) and region B (*α*-methylene-*γ*-lactone) are crucial for the inhibition of NF-κB or STAT3 signaling pathway. Region C and region D are available sites for structure modification without undermining its biological activity.

conjugation with functional groups to improve the activity [14–16].

2.6. *Anticancer mechanism of compound **43***

To further elucidate the anticancer mechanism of compound **43**, its induction of cell apoptosis was studied by Annexin V/PI staining of **43**-incubated human glioblastoma U87MG cells. The results at 12 h after the treatment of compound **43** at different concentrations were shown in Fig. 8 and the percentage of apoptotic (early and late stage) cells were showed in Fig. 9. Groups treated with compound **43** showed a higher portion of apoptotic cells compared with the control group, indicating that compound **43** exhibited an induction effect on cell apoptosis.

Based on the above-mentioned *in vivo* results, it could be concluded that compound **43** showed high promise as an anticancer clinical drug candidate. The elucidation of its anticancer mechanism is of great significance for the ultimate discovery of anticancer drugs derived from PTL or MCL. Cytotoxic drugs, such as paclitaxel or doxorubicin, usually exhibit high activity in growth inhibition or apoptosis induction [42–44]. In contrast, immune modulator compounds such as parthenolide (**1**) and micheliolide (**3**) were relatively less active in terms of cytotoxicity or promoting cell apoptosis as reported by previous studies [11,19,27]. In this study, although compound **43** showed strong

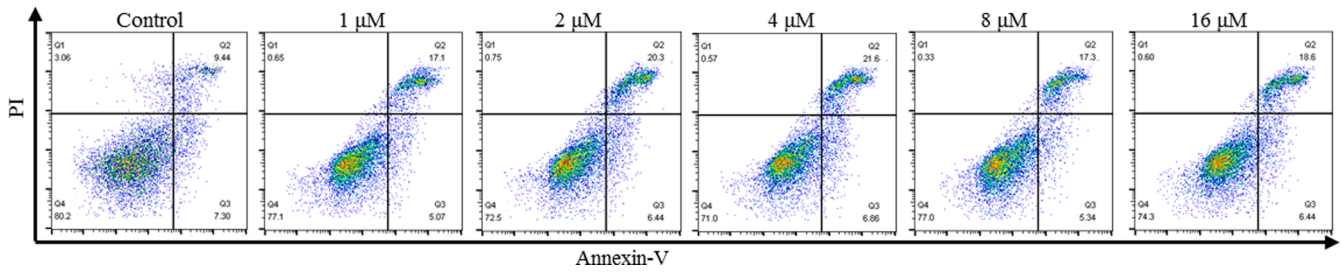

Fig. 8. Apoptosis in U87MG cells after then treatment of compound **43**.

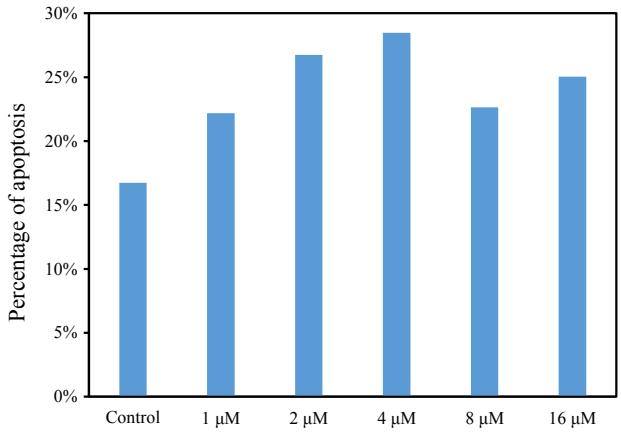

Fig. 9. The percentage of apoptotic cells (early and late stage) in U87MG cells treated by compound **43**.

anticancer activity comparable to clinical drugs in multiple *in vivo* assays, compound **43** showed moderate cytotoxicity (Table 1) and moderate apoptosis induction ability (Fig. 8) compared with cytotoxic compounds. Accordingly, based on the inhibition effect of compound **43** toward NF-κB and STAT3 signaling pathways, it could be postulated that compound **43** is more likely to be the modulator of the immune system rather than a cytotoxic compound. The anticancer activity of compound **43** largely stems from its inhibition effect toward NF-κB and STAT3 signaling pathways, which regulates the immune responses *in vivo* and decrease the survivability of tumor cells.

3. Conclusion

In this study, thirteen novel parthenolide derivatives and twenty-three novel micheliolide derivatives were synthesized. Synthesized compounds were evaluated for their anticancer activity in multiple *in vitro* and *in vivo* assays. Both *in vitro* and *in vivo* results demonstrated that the modification at C-9 position of MCL was an effective way to enhance the biological activity of MCL. One MCL derivative (9-oxomicheliolide, **43**) showed strong anticancer activity toward glioblastoma in mice, with its tumor inhibition rate comparable to clinical drug temozolomide. The anticancer mechanism was then investigated, and compound **43** showed apparent inhibition effects toward NF-κB and STAT3 signaling pathways, likely owing to its α,β-unsaturated carbonyl groups. It was proposed that the biological activity of compound **43** resulted from its regulatory effect on immune responses against tumor cells by inhibiting NF-κB and STAT3 signaling pathways. Based on this work, compound **43**, 9-oxomicheliolide, presents high promise as a clinical drug candidate for glioblastoma and will be studied further in the future.

4. Experimental section

4.1. Chemistry

All chemicals were purchased from Innochem, Alladin, Adamas, Alfa, or other chemical companies. All chemicals were used without further purification unless otherwise mentioned. Thin layer chromatography (TLC) was run on silica gel plates (GF254) from Qingdao Haiyang. Nuclear magnetic resonance (NMR) was performed on Bruker AV 400 or 500 MHz (Bruker Company, USA) with tetramethylsilane as internal reference. High resolution mass chromatography was performed on Agilent 6224 TOF LC/MS with an ESI source.

4.1.1. General synthesis procedures of PTL esters 6–18

Typically, 5 mmol of PTL (**1**), 2 mmol of SeO_2, and 1.4 mL of 70% *tert*-butyl hydroperoxide (*t*-BuOOH) in H_2O were added in 70 mL of dichloromethane (DCM). The reaction mixture was stirred at 45 °C for 4 h, and then filtered with kieselguhr. The filtrate was concentrated under reduced pressure, followed by column chromatography with petroleum ether/ethyl acetate to afford pure MMB (**5**) with the yield of 47%. ^{1}H NMR (400 MHz, $CDCl_3$) δ 6.24 (d, J = 3.6 Hz, 1H, =C—H, H-13), 5.65 (d, J = 8.0 Hz, 1H, =C—H, H-1), 5.55 (d, J = 3.6 Hz, 1H, =C—H, H-13), 4.16 (d, J = 12.5 Hz, 1H, =C—C—H, H-14), 4.10 (d, J = 12.5 Hz, 1H, =C—C—H, H-14), 3.86 (t, J = 9.4 Hz, COO—C—H, H-6), 3.01–2.73 (m, 2H, =C—C—H, H—C—O-, H-7, H-5), 2.56–2.07 (m, 6H, —CH_2—, H-2, H-3, H-8, H-9), 1.76–1.62 (m, 1H, —CH_2—, H-8), 1.55 (s, 3H, —CH_3, H-15), 1.48 (s, 1H, —OH), 1.22–0.91 (m, 1H, —CH_2—, H-3). HRMS (ESI) m/z calcd for $C_{15}H_{21}O_4$ $[M + H]^+$ 265.1434, found 265.1426.

To a solution of carboxylic acid (1 mmol) in 5 mL of dimethyl sulfoxide (DMSO), 1 mmol of MMB (**5**), 3 mmol of 1-ethyl-3-(3-dimethylaminopropyl) carbodiimide hydrochloride (EDCI) and 0.3 mmol of 4-dimethylaminopyridine were added and stirred at room temperature for 4 h. After reaction was complete monitored by TLC, water was added to the solution and the mixture was extracted with ethyl acetate for three times. The organic phase was combined, washed by saturated $NaHCO_3$ and brine solution, and dried with anhydrous Na_2SO_4 overnight. The solution was then concentrated and purified by column chromatography with petroleum ether/ethyl acetate to afford compounds **6**–**18** (yield: 16–79%).

4.1.1.1. ((1aR,7aS,10aS,10bS,E)-1a-methyl-8-methylene-9-oxo-1a,2,3,6,7,7a,8,9,10a,10b-decahydrooxireno[2′,3′:9,10]cyclodeca[1,2-b]furan-5-yl)methyl 5-nitrofuran-2-carboxylate (6). White solid; yield 27%. ^{1}H NMR (400 MHz, $CDCl_3$) δ 7.35 (d, J = 3.7 Hz, 1H, Ar—H), 7.31 (d, J = 3.7 Hz, 1H, Ar—H), 6.25 (d, J = 3.5 Hz, 1H, =C—H, H-13), 5.83 (d, J = 8.0 Hz, 1H, =C—H, H-1), 5.56 (d, J = 3.5 Hz, 1H, =C—H, H-13), 4.96 (d, J = 12.2 Hz, 1H, =C—C—H, H-14), 4.75 (d, J = 12.2 Hz, 1H, =C—C—H, H-14), 3.87 (t, J = 9.3 Hz, 1H, COO—C—H, H-6), 2.95–2.82 (m, 2H, =C—C—H, H—C—O-, H-7,H-5), 2.58–2.15(m, 6H, —CH_2—, H-2, H-3, H-8, H-9), 1.77–1.70 (m, 1H, —CH_2—, H-8), 1.56 (s, 3H, —CH_3, H-15), 1.17–1.10 (m, 1H, —CH_2—, H-3). ^{13}C NMR (126 MHz, $CDCl_3$) δ (100 MHz, $CDCl_3$) δ 169.19, 156.63, 152.36, 144.29, 138.53, 133.85, 132.22, 120.24, 119.24, 111.70, 80.83, 68.13, 63.09, 59.90, 42.52,

36.34, 25.44, 24.20, 23.77, 17.84. HRMS (ESI) *m/z* calcd for $C_{20}H_{22}0_8N$ $[M + H]^+$ 404.1340, found 404.1333.

*4.1.1.2. ((1aR,7aS,10aS,10bS,E)-1a-methyl-8-methylene-9-oxo-1a,2,3,6,7,7a,8,9,10a,10b-decahydrooxireno[2′,3′:9,10]cyclodeca[1,2-b]furan-5-yl)methyl 9,10-dioxo-9,10-dihydroanthracene-2-carboxylate (**7**).* Light green solid; yield 16%. ^{1}H NMR (400 MHz, $CDCl_3$) δ 8.92–8.90 (m, 1H, Ar—H), 8.43–8.37 (m, 2H, Ar—H), 8.35–8.30 (m, 2H, Ar—H), 7.86–7.80 (m, 2H, Ar—H), 6.24 (d, J = 3.2 Hz, 1H, =C—H, H-13), 5.83 (t, J = 8.3 Hz, 1H, =C—H, H-1), 5.56 (d, J = 3.2 Hz, 1H, =C—H, H-13), 4.99 (d, J = 12.4 Hz, 1H, =C—C—H, H-14), 4.77 (d, J = 12.4 Hz, 1H, =C—C—H, H-14), 3.86 (t, J = 9.3 Hz, 1H, COO—C—H, H-6), 2.94–2.85 (m, 2H, =C—C—H, H—C—O-, H-7, H-5), 2.55–2.14 (m, 6H, —CH_2—, H-2, H-3, H-8, H-9), 1.77–1.68 (m, 1H, —CH_2—, H-8), 1.55 (s, 3H, —CH_3, H-15), 1.19–1.06 (m, 1H, —CH_2—, H-3).^{13}C NMR (126 MHz, $CDCl_3$) δ 182.69, 182.52, 169.48, 165.00, 138.69, 136.50, 134.99, 134.85, 134.83, 134.79, 134.68, 133.81, 133.57, 133.55, 131.86, 128.80, 127.95, 127.712, 127.707, 120.83, 81.15, 67.97, 63.53, 60.20, 42.89, 36.76, 25.88, 24.46, 24.13, 18.23. HRMS (ESI) *m/z* calcd for $C_{30}H_{27}O_7$ $[M + H]^+$ 499.1751, found 499.1751

*4.1.1.3. ((1aR,7aS,10aS,10bS,E)-1a-methyl-8-methylene-9-oxo-1a,2,3,6,7,7a,8,9,10a,10b-decahydrooxireno[2′,3′:9,10]cyclodeca[1,2-b]furan-5-yl)methyl 2-phenylquinoline-4-carboxylate (**8**).* White solid; yield 36%. ^{1}H NMR (400 MHz, $CDCl_3$) δ 8.73 (dd, J = 8.6, 0.9 Hz, 1H, Ar—H), 8.45–8.35 (m, 2H, Ar—H), 8.26–8.14 (m, 2H, Ar—H), 7.86–7.81 (m, 1H), 7.71–7.66 (m, 1H, Ar—H), 7.61–7.51 (m, 3H, Ar—H), 6.23 (d, J = 3.2 Hz, 1H, =C—H, H-13), 5.87 (t, J = 8.3 Hz, 1H, =C—H, H-1), 5.54 (d, J = 3.2 Hz, 1H, =C—H, H-13), 5.09 (d, J = 12.5 Hz, 1H, =C—C—H, H-14), 4.90 (d, J = 12.5 Hz, 1H, =C—C—H, H-14), 3.89 (t, J = 9.3 Hz, 1H, COO—C—H, H-6), 2.99–2.91 (m, 2H, =C—C—H, H—C—O-, H-7, H-5), 2.67–2.13 (m, 6H, —CH_2—, H-2, H-3, H-8, H-9), 1.80–1.71 (m, 1H, —CH_2——CH_2—, H-8), 1.58 (s, 3H, —CH_3, H-15), 1.20–1.12 (m, 1H, —CH_2—, H-3).^{13}C NMR (126 MHz, $CDCl_3$) δ 169.40, 166.25, 156.93, 138.82, 138.64, 135.61, 134.62, 131.48, 130.57, 130.40, 130.13, 129.24, 128.28, 127.70, 125.36, 120.71, 120.48, 81.14, 67.93, 63.51, 60.16, 42.84, 36.79, 25.92, 24.57, 24.13, 18.22. HRMS (ESI) *m/z* calcd for $C_{31}H_{30}O_5N$ $[M + H]^+$ 496.2118, found 496.2111.

*4.1.1.4. ((1aR,7aS,10aS,10bS,E)-1a-methyl-8-methylene-9-oxo-1a,2,3,6,7,7a,8,9,10a,10b-decahydrooxireno[2′,3′:9,10]cyclodeca[1,2-b]furan-5-yl)methyl 4-oxo-4H-chromene-2-carboxylate (**9**).* Light green solid; yield 22%. ^{1}H NMR (500 MHz, $CDCl_3$) δ 8.34 (d, J = 8.0 Hz, 1H, Ar—H), 7.92–7.88 (m, Ar—H), 7.72 (d, J = 8.0 Hz, 1H, Ar—H), 7.63–7.60 (m, Ar—H), 7.41 (s, 1H, Ar—H), 6.38 (s, 1H, =C—H, H-13), 5.99 (t, J = 8.0 Hz, 1H, =C—H, H-1), 5.71 (s, 1H, =C—H, H-13), 5.10 (d, J = 12.2 Hz, 1H, =C—C—H, H-14), 4.96 (d, J = 12.2 Hz, 1H, =C—C—H , H-14), 4.02 (t, J = 9.2 Hz, 1H, COO—C—H, H-6), 3.11–3.01 (m, 2H, =C—C—H, H—C—O-, H-7, H-5), 2.69–2.32 (m, 6H, —CH_2—, H-2, H-3, H-8, H-9), 1.93–1.88 (m, 1H, —CH_2—, H-8), 1.72 (s, 3H, —CH_3, H-15), 1.29 (t, J = 13.1 Hz, 1H, —CH_2—, H-3). ^{13}C NMR (126 MHz, $CDCl_3$) δ 178.49, 169.39, 160.54, 156.10, 151.86, 138.69, 135.20, 133.96, 132.88, 126.34, 125.97, 124.56, 120.76, 118.97, 115.31, 81.05, 69.04, 63.46, 60.16, 42.88, 36.66, 25.78, 24.47, 24.12, 18.21. HRMS (ESI) *m/z* calcd for $C_{25}H_{25}O_7$ $[M + H]^+$437.1578, found 437. 1595.

*4.1.1.5. ((1aR,7aS,10aS,10bS,E)-1a-methyl-8-methylene-9-oxo-1a,2,3,6,7,7a,8,9,10a,10b-decahydrooxireno[2′,3′:9,10]cyclodeca[1,2-b]furan-5-yl)methyl 3-(2-chloroacetamido)benzoate (**10**).* White solid; yield 61%. ^{1}H NMR (500 MHz, $CDCl_3$) δ 8.31 (s, 1H, N—H), 8.17 (s, 1H, Ar—H), 7.90–7.73 (m, 2H, Ar—H), 7.50–7.42 (m, 1H, Ar—H), 6.20 (s, 1H, =C—H, H-13), 5.79 (d, J = 8.0 Hz, 1H, =C—H, H-1), 5.48 (s, 1H, =C—H, H-13), 4.90 (d, J = 12.4 Hz, 1H, =C—C—H, H-14), 4.74 (d, J = 12.4 Hz, 1H, =C—C—H, H-14), 4.22 (d, J = 5.9 Hz, 2H, —CH_2—Cl), 3.87 (t, J = 9.2 Hz, 1H, COO—C—H, H-6), 3.08–2.96 (m, 1H, =C—C—H, H-7), 2.92 (d, J = 9.2 Hz, 1H, H—C—O-, H-5), 2.58–2.15 (m, 6H, —CH_2—, H-2, H-3, H-8, H-9), 1.73–1.68 (m, 1H, —CH_2—, H-8), 1.56 (s, 3H, —CH_3, H-15), 1.15 (t, J = 13.0 Hz, 1H, —CH_2—, H-3). ^{13}C NMR (126 MHz, $CDCl_3$) δ 169.44, 165.69, 164.13, 138.69, 137.06, 134.77, 131.32, 130.72, 129.43, 126.27, 124.69, 120.90, 120.38, 80.99, 67.67, 63.32, 59.99, 42.85, 42.76, 36.57, 25.84, 24.75, 23.90, 18.02. HRMS (ESI) *m/z* calcd for $C_{24}H_{27}O_6NCl$ $[M + H]^+$ 460.1521, found 460.1510.

*4.1.1.6. ((1aR,7aS,10aS,10bS,E)-1a-methyl-8-methylene-9-oxo-1a,2,3,6,7,7a,8,9,10a,10b-decahydrooxireno[2′,3′:9,10]cyclodeca[1,2-b]furan-5-yl)methyl 2-(4-chlorophenoxy)acetate (**11**).* White solid; yield 51%. ^{1}H NMR (500 MHz, $CDCl_3$) δ 7.26 (d, J = 8.0 Hz, 2H, Ar—H), 6.83 (d, J = 8.0 Hz, 2H, Ar—H), 6.25 (s, 1H, =C—H, H-13), 5.68 (d, J = 7.4 Hz, 1H, =C—H, H-1), 5.51 (s, 1H, =C—H, H-13), 4.77 (d, J = 12.2 Hz, 1H, =C—C—H, H-14), 4.65–4.53 (m, 3H, =C—C—H, —OOC—CH_2—, H-14), 3.83 (t, J = 9.1 Hz, 1H,COO—C—H, H-6), 2.85–2.78 (m, 2H,=C—C—H,H—C—O-, H-7, H-5), 2.45–2.16 (m, 6H, —CH_2—, H-2, H-3, H-8, H-9), 1.66–1.58 (m, 1H, —CH_2—, H-8), 1.54 (s, 3H, —CH_3, H-15), 1.09 (t, J = 12.7 Hz, 1H, —CH_2—, H-3). ^{13}C NMR (126 MHz, $CDCl_3$) δ 169.24, 168.44, 156.22, 138.56, 134.19, 131.83, 129.52, 126.88, 120.38, 115.86, 80.86, 67.47, 65.44, 63.20, 59.89, 42.60, 36.47, 25.47, 24.20, 23.82, 17.96. HRMS (ESI) *m/z* calcd for $C_{23}H_{26}O_6Cl$ $[M + H]^+$ 433.1412, found 433.1406.

*4.1.1.7. ((1aR,7aS,10aS,10bS,E)-1a-methyl-8-methylene-9-oxo-1a,2,3,6,7,7a,8,9,10a,10b-decahydrooxireno[2′,3′:9,10]cyclodeca[1,2-b]furan-5-yl)methyl 2-((4-fluorophenyl)thio)acetate (**12**).* White solid; yield 56%. ^{1}H NMR (400 MHz,DMSO-d_6) δ 7.55–7.37 (m, 2H, Ar—H), 7.27–7.17 (m, 2H, Ar—H), 6.03 (d, J = 3.5 Hz, 1H, =C—H, H-13), 5.53–5.51 (m, 2H, =C—H, H-1, H-13), 4.59 (d, J = 12.6 Hz, 1H, =C—C—H, H-14), 4.41 (d, J = 12.6 Hz, 1H, =C—C—H, H-14), 4.07 (t, J = 9.4 Hz, 1H, COO—C—H, H-6), 3.89 (s, 2H, S—C—H), 3.03–2.84 (m, 1H, =C—C—H, H-7), 2.77 (d, J = 9.4 Hz, 1H, H—C—O—, H-5), 2.30–2.01 (m, 6H, —CH_2—, H-2, H-3, H-8, H-9), 1.59–1.52 (m, 1H, —CH_2—, H-8), 1.45 (s, 3H, —CH_3, H-15), 0.91–0.76 (m, 1H, —CH_2—, H-3). ^{13}C NMR (126 MHz, DMSO-d_6) δ 170.04, 169.73, 140.27, 135.23, 132.05, 131.98, 130.18, 119.86, 116.85, 116.68, 81.22, 67.87, 63.22, 60.60, 42.34, 36.88, 36.12, 25.13, 24.28, 23.80, 18.07. HRMS (ESI) *m/z* calcd for $C_{23}H_{26}O_5FS$ $[M + H]^+$ 433.1479, found 433.1473.

*4.1.1.8. ((1aR,7aS,10aS,10bS,E)-1a-methyl-8-methylene-9-oxo-1a,2,3,6,7,7a,8,9,10a,10b-decahydrooxireno[2′,3′:9,10]cyclodeca[1,2-b]furan-5-yl)methyl 4-(4-bromophenyl)-4-oxobutanoate (**13**).* Orange solid; yield 56%. ^{1}H NMR (400 MHz, $CDCl_3$) δ 7.83 (d, J = 8.4 Hz, 2H, Ar—H), 7.62 (d, J = 8.4 Hz, 2H, Ar—H), 6.24 (d, J = 3.0 Hz, 1H, =C—H, H-13), 5.70 (t, J = 7.8 Hz, 1H, =C—H, H-1), 5.59 (d, J = 3.0 Hz, 1H, =C—H, H-13), 4.71 (d, J = 12.4 Hz, 1H, =C—C—H, H-14), 4.48 (d, J = 12.4 Hz, 1H, =C—C—H, H-14), 3.85 (t, J = 9.3 Hz, 1H, COO—C—H, H-6), 3.28 (t, J = 6.2 Hz, 2H, —OOC—C—H), 2.96–2.73 (m, 4H, —OOC—C—H, =C—C—H,H—C—O—, H-5, H-7), 2.48–2.13 (m, 6H, —CH_2—, H-2, H-3, H-8, H-9), 1.70–1.64 (m, 1H, —CH_2—, H-8), 1.55 (s, 3H, —CH_3, H-15), 1.11 (t, J = 12.9 Hz, 1H, —CH_2—, H-3). ^{13}C NMR (126 MHz, $CDCl_3$) δ 197.32, 172.85, 169.79, 138.73, 135.05, 134.84, 132.00, 130.75, 129.51, 128.59, 120.36, 81.03, 67.20, 63.27, 59.93, 42.68, 36.59, 33.24, 28.04, 25.74, 24.52, 23.83, 18.01. HRMS (ESI) *m/z* calcd for $C_{25}H_{28}O_6Br$ $[M + H]^+$ 503.1064, found 503.1057.

*4.1.1.9. ((1aR,7aS,10aS,10bS,E)-1a-methyl-8-methylene-9-oxo-1a,2,3,6,7,7a,8,9,10a,10b-decahydrooxireno[2′,3′:9,10]cyclodeca[1,2-b]furan-5-yl)methyl 3-(1,3-dioxo-1H-benzo[de]isoquinolin-2(3H)-yl)propanoate (**14**).* Light yellow solid; yield 29%. ^{1}H NMR (400 MHz, $CDCl_3$) δ 8.59 (d, J = 7.0 Hz, 2H, Ar—H), 8.24 (d, J = 8.0 Hz, 2H, Ar—H), 7.79–7.76 (m, 2H, Ar—H), 6.25 (s, 1H, =C—H, H-13), 5.77–5.57 (m, 2H, =C—H, H-1, H-13), 4.69–4.43 (m, 4H, N—CH_2—, =C—C—H, H-14), 3.81 (t, J = 9.2 Hz, 1H, COO—C—H, H-6), 2.85–2.76 (m, 3H,

=C—C—H, —OOC—C—H, H-7), 2.69–2.65 (m, 1H, H—C—O-, H-5), 2.46–2.04 (m, 6H, —CH_2—, H-2, H-3, H-8, H-9), 1.64–1.62 (m, 1H, —CH_2—, H-8), 1.52 (s, 3H, —CH_3, H-15), 1.00 (t, J = 12.1 Hz, 1H, —CH_2—, H-3). ^{13}C NMR (126 MHz, $CDCl_3$) δ 171.30, 169.62, 164.27, 138.89, 134.88, 134.53, 131.84, 131.64, 131.09, 128.35, 127.25, 122.51, 120.70, 81.13, 67.52, 63.39, 60.11, 42.87, 36.69, 36.44, 33.09, 25.97, 24.71, 23.98, 18.19. HRMS (ESI) *m/z* calcd for $C_{30}H_{30}O_7N$ $[M + H]^+$ 516.2017, found 516.2012.

4.1.1.10. ((1aR,7aS,10aS,10bS,E)-1a-methyl-8-methylene-9-oxo-1a,2,3,6,7,7a,8,9,10a,10b-decahydrooxireno[2′,3′:9,10]cyclodeca[1,2-b]furan-5-yl)methyl 3-(6,7-dimethoxy-3,4-dihydroisoquinolin-2(1H)-yl)propanoate ***(15)***. White solid; yield 34%.^{1}H NMR (400 MHz,$CDCl_3$) δ 6.59 (s, 1H, Ar—H), 6.49 (s, 1H, Ar—H), 6.25 (d, J = 3.2 Hz, 1H, =C—H, H-13), 5.72 (t, J = 8.2 Hz, 1H, =C—H, H-1), 5.56 (d, J = 3.2 Hz, 1H, =C—H, H-13), 4.75 (d, J = 12.4 Hz, 1H, =C—C—H, H-14), 4.53 (d, J = 12.4 Hz, 1H, =C—C—H, H-14), 3.88–3.82 (m, 7H, —O—CH_3, COO—C—H, H-6), 3.74 (s, 2H, N—CH_2—), 3.45–3.40 (m, 2H, =C—C—H, —OOC—C—H, H-7, H-5), 2.94–2.83 (m, 6H, —CH_2—, H-2, H-3, H-8, H-9), 2.52–1.99 (m, 8H, Ar—CH_2—, N—CH_2—, —OOC—CH_2—), 1.74–1.63 (m, 1H, —CH_2—, H-8), 1.55 (s, 3H, —CH_3, H-15), 1.14–1.08 (m, 1H, —CH_2—, H-3). ^{13}C NMR (126 MHz, $CDCl_3$) δ 170.02, 169.30, 147.59, 147.24, 138.65, 134.62, 131.21, 125.44, 123.57, 120.40, 111.24, 109.18, 80.96, 66.83, 63.24, 59.92, 58.57, 55.89, 55.86, 54.92, 50.78, 42.62, 36.55, 28.23, 25.70, 24.42, 23.84, 17.99. HRMS (ESI) *m/z* calcd for $C_{29}H_{38}O_7N$ $[M + H]^+$ 512.2643, found 512.2604.

4.1.1.11. ((1aR,7aS,10aS,10bS,E)-1a-methyl-8-methylene-9-oxo-1a,2,3,6,7,7a,8,9,10a,10b-decahydrooxireno[2′,3′:9,10]cyclodeca[1,2-b]furan-5-yl)methyl 2-(1,3-dioxoisoindolin-2-yl)acetate ***(16)***. White solid; yield 40%.^{1}H NMR (400 MHz, $CDCl_3$) δ 7.90 (dd, J = 5.5, 3.0 Hz, 2H, Ar—H), 7.77 (dd, J = 5.5, 3.0 Hz, 2H, Ar—H), 6.25 (d, J = 3.2 Hz, 1H, =C—H, H-13), 5.71 (t, J = 8.1 Hz, 1H, =C—H, H-1), 5.57 (d, J = 3.2 Hz, 1H, =C—H, H-13), 4.76 (d, J = 12.4 Hz, 1H, =C—C—H, H-14), 4.55 (d, J = 12.4 Hz, 1H, =C—C—H, H-14), 4.45 (d, J = 2.1 Hz, 2H, N—CH_2—), 3.83 (t, J = 9.3 Hz, 1H, COO—C—H, H-6), 2.86–2.80 (m, 2H, =C—C—H, H—C—O—, H-7, H-5), 2.43–2.19 (m, 6H, —CH_2—, H-2, H-3, H-8, H-9), 1.83–1.61 (m, 1H, —CH_2—, H-8), 1.54 (s, 3H, —CH_3, H-15), 1.15–1.07 (m, 1H, —CH_2—, H-3). ^{13}C NMR (126 MHz, $CDCl_3$) δ 169.34, 167.45, 167.14, 138.65, 134.45, 134.28, 131.95, 131.69, 123.74, 120.47, 80.99, 68.07, 63.29, 59.92, 42.66, 38.95, 36.57, 25.64, 24.34, 23.88, 18.02. HRMS (ESI) *m/z* calcd for $C_{25}H_{26}O_7N$ $[M + H]^+$ 452.1704, found 452.1673.

4.1.1.12. ((1aR,7aS,10aS,10bS,E)-1a-methyl-8-methylene-9-oxo-1a,2,3,6,7,7a,8,9,10a,10b-decahydrooxireno[2′,3′:9,10]cyclodeca[1,2-b]furan-5-yl)methyl 4-(5-(bis(2-chloroethyl)amino)-1-methyl-1H-benzo[d]imidazol-2-yl)butanoate ***(17)***. White solid; yield 40%. ^{1}H NMR (400 MHz,$CDCl_3$) δ 7.39 (d, J = 10 Hz, 1H, Ar—H), 6.96 (s, 1H, Ar—H), 6.83 (d, J = 10 Hz, 1H, Ar—H), 6.07 (d, J = 3.5 Hz, 1H, =C—H, H-13), 5.70–5.60 (m, 2H, H-1, =C—H, H-13), 4.63 (d, J = 12.4 Hz, 1H, =C—C—H), 4.47 (d, J = 12.4 Hz, 1H, =C—C—H), 3.83–3.72 (m, 9H, N—CH_2—, Cl—CH_2—, H-6), 3.70 (s, 3H, N—CH_3), 3.07–2.97 (m, 1H, =C—C—H, H-7), 2.91–2.84 (m, 3H, N=C—CH_2—, H—C—O-, H-5), 2.43–1.98 (m, 10*H*, —OOC—CH_2—, H-2, H-3, H-8, H-9), 1.71–1.61 (m, 1H, —CH_2—, H-8), 1.51 (s, 3H, —CH_3, H-15), 1.01–0.94 (m, 1H, H-3). ^{13}C NMR (126 MHz, DMSO-d_6) δ 173.17, 170.11, 154.83, 143.02, 140.24, 135.66, 130.00, 129.69, 129.33, 120.15, 111.00, 110.56, 81.30, 67.03, 63.28, 60.66, 54.02, 42.45, 42.05, 36.95, 33.40, 31.37, 30.12, 26.17, 25.32, 24.53, 23.86, 22.68, 18.11. HRMS (ESI) *m/z* calcd for $C_{31}H_{40}O_5N_3Cl_2$ $[M + H]^+$ 604.2340, found 604.2339.

4.1.1.13. 4-(2-((4-(((1aR,7aS,10aS,10bS,E)-1a-methyl-8-methylene-9-oxo-1a,2,3,6,7,7a,8,9,10a,10b-decahydrooxireno[2′,3′:9,10]cyclodeca[1,2-b]furan-5-yl)methoxy)-4-oxobutanoyl)oxy)ethoxy)-3-(phenylsulfonyl)-1,2,5-oxadiazole 2-oxide ***(18)***. White solid; yield 79% .^{1}H NMR (500 MHz, DMSO-d_6) δ 8.06 (d, J = 7.6 Hz, 2H, Ar—H), 7.91–7.88 (m, 1H, Ar—H), 7.78–7.71 (m, 2H, Ar—H), 6.08 (d, J = 2.7 Hz, 1H, =C—H, H-13), 5.66–5.61 (m, 2H, =C—H, H-13, H-1), 4.63–4.60 (m, 3H, =C—C—H, H—C—O-, H-14), 4.43–4.41 (m, 3H, =C—C—H, H—C—O—), 4.12 (t, J = 9.2 Hz, 1H, COO—C—H, H-6), 3.00–2.95 (m, 1H, =C—C—H, H-7), 2.87 (d, J = 9.2 Hz, 1H, H—C—O—, H-5), 2.66 (s, 4H, —OOC—C—H), 2.35–2.05 (m, 6H, —CH_2—, H-2, H-3, H-8, H-9), 1.66–1.62 (m, 1H, —CH_2—, H-8), 1.46 (s, 3H, —CH_3, H-15), 0.95–0.90 (m, 1H, —CH_2—, H-3). ^{13}C NMR (126 MHz, DMSO-d_6) δ 172.63, 172.45, 170.09, 159.35, 140.28, 137.82, 136.83, 135.53, 130.67, 129.95, 129.02, 120.01, 111.14, 81.29, 69.89, 67.31, 63.27, 62.21, 60.63, 42.45, 36.93, 29.20, 29.17, 25.26, 24.46, 23.84, 18.11. HRMS (ESI) *m/z* calcd for $C_{29}H_{33}O_{12}N_2S$ $[M + H]^+$ 633.1749, found 633.1743.

4.1.2. Synthesis procedures of compound ***3***

50 mmol of PTL (**1**) dissolved in dichloromethane (18 mL) was added dropwise to a solution of *p*-toluenesulfonic acid (344 mg, 2.0 mmol) in 80 mL dichloromethane. The reaction mixture was stirred at room temperature overnight. After all PTL was converted, $NaHCO_3$ solution was added to the reaction solution. The reaction mixture was stirred for 1 h. The organic phase from the mixture was washed with saturated brine twice, and then concentrated to crude MCL (**3**) as yellow solid. The crude product was recrystallized from acetone to give compound **3** (10.2 g) as pale yellow solid with the yield being 82%. ^{1}H NMR ($CDCl_3$, 500 MHz) δ 6.21 (d, J = 3.5 Hz, 1H, H-13), 5.50 (d, J = 3.5 Hz, 1H, H-13), 3.82 (t, J = 10.4 Hz, 1H, H-6), 2.74 (d, J = 10.2 Hz, 1H, H-5), 2.67 (t, J = 11.1 Hz, 1H, H-7), 2.42–2.37 (m, 1H), 2.27–2.21 (m, 3H), 2.12–2.07 (d, J = 13.8 Hz, 1H), 1.73–1.86 (m, 2H), 1.68 (s, 3H), 1.36–1.28 (m, 4H).

4.1.3. Synthesis procedures of compounds ***19–21***

1.0 mmol of MCL (**3**), 0.3 mmol of SeO_2 and 0.28 mL of 70% *t*-BuOOH/H_2O were added to 30 mL of dichloromethane. The mixture was stirred and refluxed for 3 h. The resulting mixture was filtered with kieselguhr, and then concentrated under vacuo. The residue was purified by silica gel column chromatography (petroleum ether: ethyl acetate = 1:1) to obtain compounds **19**, **20**, and **21**, with the yield of 53%, 14%, and 7%. Compound **20** has been reported by a previous research [6], while compounds **19** and **21** are first reported in this literature.

4.1.3.1. (3aS,5S,9R,9aS,9bS)-5,9-dihydroxy-6,9-dimethyl-3-methylene-3a,4,5,7,8,9,9a,9b-octahydroazuleno[4,5-b]furan-2(3H)-one ***(19)***. Yellow solid; yield 53%. ^{1}H NMR (500 MHz, $CDCl_3$): δ 6.24 (d, J = 3.4 Hz, 1H, H-13), 5.55 (d, J = 3.4 Hz, 1H, H-13), 4.38–4.36 (m, 1H, H-9), 4.04 (s, 1H, OH), 3.88 (t, J = 8.0 Hz, 1H, H-6), 3.37 (t, J = 8.0 Hz, 1H, H-7), 2.91 (d, J = 12.8 Hz, 1H, H-5), 2.44–2.23 (m, 3H), 1.89–1.81 (m, 5H), 1.63–1.56 (m, 1H, H-8), 1.32 (s, 3H, H-15). ^{13}C NMR (126 MHz, $CDCl_3$): δ 169.94, 138.43, 135.74, 132.68, 120.07, 83.85, 80.84, 72.63, 57.80, 41.37, 37.67, 33.04, 30.53, 22.76, 22.42. HRMS (ESI) *m/z* calcd for $C_{15}H_{20}O_4$ $[M + Na]^+$ 287.1254, found 287.1237.

4.1.3.2. (1R,3aR,4aS,6aS,9aS,9bS)-1-hydroxy-1,4a-dimethyl-7-methyleneoctahydro-1H-oxireno[2′,3′:8,8a]azuleno[4,5-b]furan-8(4aH)-one ***(20)***. White solid; yield 14%. ^{1}H NMR (400 MHz, $CDCl_3$): δ 6.19 (d, J = 3.3 Hz, 1H, H-13), 5.48 (d, J = 3.3 Hz, 1H,H-13), 4.05 (t, J = 10.3 Hz, 1H, H-6), 2.36–2.22 (m, 4H), 2.02–1.80 (m, 4H), 1.70–1.61 (m, 1H), 1.47 (s, 3H), 1.43–1.40 (m, 1H), 1.30 (s, 3H).

4.1.3.3. (3aS,6R,9R,9aS,9bS)-6,9-dihydroxy-6,9-dimethyl-3-methylene-3a,4,5,6,8,9,9a,9b-octahydroazuleno[4,5-b]furan-2(3H)-one ***(21)***. White solid; yield 7%. ^{1}H NMR (500 MHz, $CDCl_3$) δ 6.18 (d, J = 3.0 Hz, 1H, H-13), 5.87–5.85 (m, 1H, H-2), 5.50 (d, J = 3.0 Hz, 1H, H-13), 4.31 (dd, J = 11.4, 9.8 Hz, 1H, H-6), 3.06 (d, J = 11.4 Hz, 1H, H-5), 2.69–2.63 (m,

1H, H-7), 2.62–2.59 (m, 1H, H-3), 2.27–2.23 (m, 1H, H-3), 2.03–1.97 (m, 2H, H-8, 9), 1.90–1.83 (m, 1H, H-8), 1.73–1.69 (m, 1H, H-9), 1.49 (s, 3H, H-14), 1.40 (s, 3H, H-15). ^{13}C NMR (126 MHz, $CDCl_3$) δ 170.07 (C-11), 146.77 (C-1), 139.16 (C-12), 125.71 (C-2), 119.32 (C-13), 82.97 (C-4), 81.50 (C-6), 70.86 (C-10), 61.63 (C-5), 49.76 (C-7), 44.93 (C-3), 38.21 (C-9), 30.05 (C-14), 23.01 (C-15), 21.79 (C-8). HRMS (ESI) *m/z* calcd for $C_{15}H_{20}O_4$ $[M + Na]^+$ 287.1259, found 287.1246.

4.1.4. General synthesis procedure for compounds **23–42**

To a solution of compound **19** (132 mg, 0.5 mmol) in CH_2Cl_2 (5 mL) was added appropriate carboxylic acid (0.6 mmol), EDCI (288 mg, 1.5 mmol), and DMAP (12 mg, 0.1 mmol). The mixture was stirred at room temperature until the disappearance of compound **19** in TLC. The mixture was then diluted with water (15 mL), and then extracted with CH_2Cl_2 (10 mL × 2). The organic layer was successively washed with saturated $NaHCO_3$ solution (10 mL × 3) and brine (10 mL × 2), and then dried over anhydrous Na_2SO_4. The solvent was removed under vacuum to get the crude product, which was purified by column chromatography to give compounds **23–42** in yield of 33–68%.

4.1.4.1. (3aS,5S,9R,9aS,9bS)-9-hydroxy-6,9-dimethyl-3-methylene-2-oxo-2,3,3a,4,5,7,8,9,9a,9b-decahydroazuleno[4,5-b]furan-5-yl 4-oxo-4H-chromene-3-carboxylate (23).

White solid; yield 41%. ^{1}H NMR (500 MHz, $CDCl_3$) δ 8.20 (d, J = 5 Hz, 1H, Ar—H), 7.76–7.70 (m, 1H, Ar—H), 7.62–7.60 (m, 1H, Ar—H), 7.48–7.45 (m, 1H, Ar—H), 7.09 (s, 1H, CO—CH), 6.27 (s, 1H, H-13), 5.74 (s, 1H, H-9), 5.53 (s, 1H, H-13), 4.31 (t, J = 6.0 Hz, 1H), 3.96 (t, J = 10.4 Hz, 1H, H-6), 3.31 (t, J = 9.2 Hz, 1H, H-7), 3.03 (d, J = 10.9 Hz, 1H, H-5), 2.64 (s, 1H, OH), 2.56–2.44 (m, 2H, H-2), 2.32–2.25 (m, 1H, H-8), 1.96–1.78 (m, 5H, H-3, H-14), 1.73–1.70 (m, 1H, H-8), 1.35 (s, 3H, H-15). ^{13}C NMR (100 MHz, $CDCl_3$) δ 178.27, 168.92, 160.15, 155.93, 151.90, 140.87, 137.87, 134.92, 128.18, 125.12, 125.81, 124.42, 120.10, 118.86, 115.15, 83.23, 80.33, 76.74, 58.20, 42.50, 37.90, 30.96, 30.68, 22.75, 22.72. HRMS (ESI) *m/z* calcd for $C_{25}H_{25}O_7$ $[M + H]^+$ 437.1595, found 437.1579.

4.1.4.2. (3aS,5S,9R,9aS,9bS)-9-hydroxy-6,9-dimethyl-3-methylene-2-oxo-2,3,3a,4,5,7,8,9,9a,9b-decahydroazuleno[4,5-b]furan-5-yl furan-2-carboxylate (24).

White solid; yield 43%. ^{1}H NMR (400 MHz, $CDCl_3$) δ 7.58 (s, 1H, Ar—H), 7.17 (d, J = 3.5 Hz, 1H, Ar—H), 6.52 (d, J = 3.5 Hz, 1H, Ar—H), 6.23 (d, J = 3.4 Hz, 1H, H-13), 5.65 (d, J = 4.9 Hz, 1H, H-9), 5.48 (d, J = 3.4 Hz, 1H, H-13), 3.92 (t, J = 10.0 Hz, 1H, H-6), 3.30 (t, J = 15.0 Hz, 1H, H-7), 3.01 (d, J = 15.0 Hz, 1H, H-5), 2.60–1.60 (m, 9H), 1.33 (s, 3H, H-15). ^{13}C NMR (100 MHz, $CDCl_3$) δ 169.23, 158.10, 146.63, 144.34, 139.40, 138.20, 129.10, 119.79, 118.43, 111.96, 83.53, 80.33, 74.17, 57.95, 42.50, 37.95, 30.76, 30.69, 22.73, 22.57. HRMS (ESI) *m/z* calcd for $C_{20}H_{23}O_6$ $[M + H]^+$ 359.1489, found 359.1486.

4.1.4.3. (3aS,5S,9R,9aS,9bS)-9-hydroxy-6,9-dimethyl-3-methylene-2-oxo-2,3,3a,4,5,7,8,9,9a,9b-decahydroazuleno[4,5-b]furan-5-yl 5-nitrofuran-2-carboxylate (25).

White solid; yield 43%. ^{1}H NMR (500 MHz, $CDCl_3$) δ 7.38 (d, J = 3.9 Hz, 1H, Ar—H), 7.34 (d, J = 4.1 Hz, 1H, Ar—H), 6.26 (s, 1H, H-13), 5.71 (s, 1H, H-9), 5.51 (s, 1H, H-13), 3.94 (t, J = 10.5 Hz, 1H, H-6), 3.27 (t, J = 11.2 Hz, 1H, H-7), 3.00 (d, J = 11.1 Hz, 1H, H-5), 2.52–2.42 (m, 2H, H-2), 2.29–2.27 (m, 1H, H-8), 1.92–1.75 (m, 6H, H-3, 8, 14), 1.34 (s, 3H, H-15). ^{13}C NMR (100 MHz, $CDCl_3$) δ 168.99, 156.52, 152.66, 144.45, 140.64, 137.91, 128.22, 120.06, 119.24, 111.49, 83.26, 80.33, 76.15, 58.15, 42.44, 37.89, 30.93, 30.73, 22.73, 14.15. HRMS (ESI) *m/z* calcd for $C_{20}H_{21}NO_8Na$ $[M + Na]^+$ 426.1263, found 426.1247.

4.1.4.4. (3aS,5S,9R,9aS,9bS)-9-hydroxy-6,9-dimethyl-3-methylene-2-oxo-2,3,3a,4,5,7,8,9,9a,9b-decahydroazuleno[4,5-b]furan-5-yl benzofuran-2-carboxylate (26).

White solid; yield 45%. ^{1}H NMR (400 MHz, $CDCl_3$) δ 7.72–7.57 (m, 2H, Ar- H), 7.53 (d, J = 0.9 Hz, 1H, Ar—H), 7.50–7.28 (m, 2H, Ar—H), 6.24 (d, J = 3.4 Hz, 1H, H-13), 5.74 (dd, J = 4.9, 2.0 Hz, 1H, H-9), 5.51 (d, J = 3.4 Hz, 1H, H-13), 3.96 (dd, J = 10.8, 10.2 Hz, 1H, H-6), 3.41–3.32 (m, 1H, H-7), 3.07 (dt, J = 11.0, 2.6 Hz, 1H, H-5), 2.64 (s, 1H, OH), 2.59–1.77 (m, 9H), 1.36 (s, 3H, H-15). ^{13}C NMR (126 MHz, $CDCl_3$) δ 169.24, 159.05, 155.82, 145.03, 139.66, 138.05, 128.96, 127.90, 126.79, 123.93, 122.87, 119.97, 114.46, 112.42, 83.49, 80.37, 74.74, 57.99, 42.52, 37.90, 30.80, 30.67, 29.69, 22.73. HRMS (ESI) *m/z* calcd for $C_{24}H_{25}O_6$ $[M + H]^+$ 409.1651, found 409.1646.

4.1.4.5. (3aS,5S,9R,9aS,9bS)-9-hydroxy-6,9-dimethyl-3-methylene-2-oxo-2,3,3a,4,5,7,8,9,9a,9b-decahydroazuleno[4,5-b]furan-5-yl 3-methylthiophene-2-carboxylate (27).

White solid; yield 38%. ^{1}H NMR (400 MHz, $CDCl_3$) δ 7.40 (d, J = 5.0 Hz, 1H, Ar—H), 6.92 (d, J = 5.0 Hz, 1H, Ar—H), 6.22 (d, J = 3.3 Hz, 1H, H-13), 5.63 (dd, J = 4.9, 1.9 Hz, 1H, H-9), 5.49 (d, J = 3.3 Hz, 1H, H-13), 4.01–3.85 (m, 1H. H-6), 3.40–3.24 (m, 1H, H-7), 3.01 (dt, J = 10.9, 2.5 Hz, 1H, H-5), 2.64 (s, 1H, OH), 2.55 (s, 3H, CH_3), 2.49–2.39 (m, 2H, H-2), 2.29–2.20 (m, 1H, H-8), 1.92–1.78 (m, 5H, H-3, H-14), 1.74–1.67 (m, 1H, H-8), 1.34 (s, 3H, H-15). ^{13}C NMR (126 MHz, $CDCl_3$) δ 169.37, 162.03, 146.56, 138.98, 138.25, 131.92, 130.57, 129.50, 126.53, 119.79, 83.61, 80.36, 73.77, 57.90, 42.72, 37.94, 30.70, 29.70, 22.70, 22.59, 16.09. HRMS (ESI) *m/z* calcd for $C_{21}H_{25}O_5S$ $[M + H]^+$ 389.1417, found 389.1414.

4.1.4.6. (3aS,5S,9R,9aS,9bS)-9-hydroxy-6,9-dimethyl-3-methylene-2-oxo-2,3,3a,4,5,7,8,9,9a,9b-decahydroazuleno[4,5-b]furan-5-yl nicotinate (28).

White solid; yield 38%. ^{1}H NMR (400 MHz, $CDCl_3$)) δ 9.21 (dd, J = 2.2, 0.9 Hz, 1H, Ar—H), 8.80 (dd, J = 4.9, 1.7 Hz, 1H, Ar—H), 8.29–8.23 (m, 1H, Ar—H), 7.41 (ddd, J = 8.0, 4.9, 0.9 Hz, 1H, Ar—H), 6.24 (d, J = 3.4 Hz, 1H, H-13), 5.74 (dd, J = 4.9, 2.1 Hz, 1H, H-9), 5.50 (d, J = 3.4 Hz, 1H, H-13), 3.95 (dd, J = 10.9, 10.1 Hz, 1H, H-6), 3.36–3.21 (m, 1H, H-7), 3.10–2.93 (m, 1H, H-5), 2.67 (s, 1H, OH), 2.56–1.72 (m, 9H), 1.35 (s, 3H, H-15). ^{13}C NMR (126 MHz, $CDCl_3$) δ 169.09, 164.61, 153.75, 150.99, 139.63, 137.99, 137.09, 128.97, 125.88, 123.41, 119.98, 83.41, 80.31, 74.82, 58.13, 42.66, 37.91, 30.80, 29.69, 22.71, 22.65. HRMS (ESI) *m/z* calcd for $C_{21}H_{24}NO_5$ $[M + H]^+$ 370.1654, found 370.1647.

4.1.4.7. (3aS,5S,9R,9aS,9bS)-9-hydroxy-6,9-dimethyl-3-methylene-2-oxo-2,3,3a,4,5,7,8,9,9a,9b-decahydroazuleno[4,5-b]furan-5-yl 2-phenylquinoline-4-carboxylate (29).

White solid; yield 38%. ^{1}H NMR (400 MHz, $CDCl_3$) δ 8.65–8.57 (m, 1H, Ar—H), 8.28 (s, 1H, Ar—H), 8.27–8.21 (m, 1H, Ar—H), 8.20–8.13 (m, 2H, Ar—H), 7.81–7.76 (m, 1H, Ar—H), 7.65–7.48 (m, 4H, Ar—H), 6.25 (d, J = 3.4 Hz, 1H, H-13), 5.91 (dd, J = 4.8, 2.2 Hz, 1H, H-9), 5.54 (d, J = 3.4 Hz, 1H, H-13), 4.02–3.97 (m, 1H, H-6), 3.34–3.28 (m, 1H, H-7), 3.05 (dt, J = 10.9, 2.5 Hz, 1H, H-5) , 2.65 (s, 1H), 2.65–2.60 (m, 2H, H-2), 2.35–2.31 (m, 1H, H-8), 1.94–1.83 (m, 6H, H-3, 8, 14), 1.37 (s, 3H, H-15). ^{13}C NMR (126 MHz, $CDCl_3$) δ 169.28, 166.29, 157.01, 149.46, 140.16, 138.86, 138.13, 136.08, 130.73, 130.28, 130.10, 129.31, 129.18, 128.11, 127.64, 125.13, 124.00, 120.33, 120.31, 83.61, 80.49, 75.67, 58.62, 42.93, 38.16, 31.08, 29.91, 23.00, 22.89. HRMS (ESI) *m/z* calcd for $C_{31}H_{30}O_5N$ $[M + H]^+$ 496.2118, found 496.2122.

4.1.4.8. (3aS,5S,9R,9aS,9bS)-9-hydroxy-6,9-dimethyl-3-methylene-2-oxo-2,3,3a,4,5,7,8,9,9a,9b-decahydroazuleno[4,5-b]furan-5-yl 3,4,5-trimethoxybenzoate (30).

White solid; yield 40%. ^{1}H NMR (400 MHz, $CDCl_3$) δ 6.24 (d, J = 3.4 Hz, 1H, H-13), 5.70 (d, J = 2.7 Hz, 1H, H-9), 5.51 (d, J = 3.4 Hz, 1H, H-13), 3.99–3.93 (m, 1H, H-6), 3.91 (s, 9H, OCH_3 × 3), 3.34–3.20 (m, 1H, H-7), 3.04–2.97 (m, 1H, H-5), 2.62 (s, 1H, OH), 2.5–2.41 (m, 2H, H-2), 2.35–2.20 (m, 1H, H-8), 1.95–1.70 (m, 6H, H-3, 8, 14), 1.36 (s, 3H, H-15). ^{13}C NMR (100 MHz, $CDCl_3$) δ 169.20, 165.57, 153.07, 142.76, 139.02, 138.15, 129.42, 124.94, 119.99, 107.10, 83.56, 80.33, 74.39, 60.99, 58.37, 56.41, 42.86, 38.00, 30.77, 22.74, 22.64. HRMS (ESI) *m/z* calcd for $C_{25}H_{31}O_8$ $[M + H]^+$ 459.2013, found 459.2011.

*4.1.4.9. (3aS,5S,9R,9aS,9bS)-9-hydroxy-6,9-dimethyl-3-methylene-2-oxo-2,3,3a,4,5,7,8,9,9a,9b-decahydroazuleno[4,5-b]furan-5-yl 2-naphthoate (**31**).* White solid; yield 40%. ^{1}H NMR (400 MHz, $CDCl_3$) δ 8.56 (s, 1H, Ar—H), 8.03–7.98 (m, 2H, Ar—H), 7.91–7.88 (m, 2H, Ar—H), 7.63–7.55 (m, 2H, Ar—H), 6.24 (d, J = 3.3 Hz, 1H, H-13), 5.78 (dd, J = 4.5, 2.0 Hz, 1H, H-9), 5.50 (d, J = 3.3 Hz, 1H, H-13), 4.00 (t, J = 15.0 Hz, 1H, H-6), 3.39 (t, J = 15.0 Hz, 1H, H-7), 3.10 (d, J = 15.0 Hz, 1H. H-5), 2.60–2.45 (m, 2H, H-2), 2.34–2.24 (m, 1H, H-8), 1.99–1.75 (m, 6H, H-3, 8, 14), 1.37 (s, 3H). ^{13}C NMR (126 MHz, $CDCl_3$) δ 169.54, 166.32, 139.28, 138.39, 135.85, 132.63, 131.44, 129.67, 129.65, 128.75, 128.61, 128.03, 127.38, 127.09, 125.35, 120.23, 83.88, 80.59, 74.50, 58.36, 42.95, 38.15, 30.99, 29.54, 22.96, 22.93. HRMS (ESI) *m/z* calcd for $C_{26}H_{27}O_5$ $[M + H]^+$ 419.1853, found 419.1836.

*4.1.4.10. (3aS,5S,9R,9aS,9bS)-9-hydroxy-6,9-dimethyl-3-methylene-2-oxo-2,3,3a,4,5,7,8,9,9a,9b-decahydroazuleno[4,5-b]furan-5-yl 1H-pyrrole-2-carboxylate (**32**).* White solid; yield 45%. ^{1}H NMR (500 MHz, $CDCl_3$) δ 9.18 (s, 1H, NH), 6.99 (s, 1H, Ar—H), 6.93(s, 1H, Ar—H), 6.29 (s, 1H, Ar—H), 6.22 (s, 1H, H-13), 5.64 (s, 1H, H-9), 5.48 (s, 1H, H-13), 3.93 (t, J = 10.6 Hz, 1H, H-6), 3.29 (t, J = 11.4 Hz, 1H, H-7), 3.01 (d, J = 11.4 Hz, 1H, H-5), 2.66 (s, 1H, OH), 2.50–2.41 (m, 2H, H-2), 2.28–2.25 (m, 1H, H-8), 1.91–1.84 (m, 2H, H-3, 8), 1.82 (s, 3H, H-14), 1.74–1.68 (m, 1H, H-3), 1.34 (s, 3H, H-15). ^{13}C NMR (126 MHz, $CDCl_3$) δ 169.56, 160.56, 139.05, 138.38, 129.57, 123.54, 122.55, 120.14, 116.06, 110.89, 83.84, 80.52, 73.58, 58.24, 42.74, 38.13, 31.02, 30.92, 22.91, 22.80. HRMS (ESI) *m/z* calcd for $C_{20}H_{24}O_5$ $[M + H]^+$ 358.1649, found 358.1666.

*4.1.4.11. (3aS,5S,9R,9aS,9bS)-9-hydroxy-6,9-dimethyl-3-methylene-2-oxo-2,3,3a,4,5,7,8,9,9a,9b-decahydroazuleno[4,5-b]furan-5-yl 1H-indole-2-carboxylate (**33**).* White solid; yield 43%. ^{1}H NMR (400 MHz, $CDCl_3$) δ 8.86 (s, 1H, NH), 7.70 (dd, J = 8.1, 1.0 Hz, 1H, Ar—H), 7.45–7.43 (m, 1H, Ar—H), 7.36–7.32 (m, 1H, Ar—H), 7.25–7.24 (m, 1H, Ar—H), 7.19–7.15 (m, 1H, Ar—H), 6.23 (d, J = 3.2 Hz, 1H,H-13), 5.72 (dd, J = 4.9, 2.1 Hz, 1H, H-9), 5.50 (d, J = 3.2 Hz, 1H, H-13), 3.99–3.94 (m, 1H, H-6), 3.37–3.32 (m, 1H, H-7), 3.09–3.06 (m, 1H, H-5), 2.56–2.43 (m, 2H, H-2), 2.30–2.27 (m, 1H, H-8), 1.95–1.72 (m, 6H, H-3, 8, 14), 1.36 (s, 3H, H-15). ^{13}C NMR (126 MHz, $CDCl_3$) δ 169.28, 161.31, 139.38, 138.09, 136.94, 129.13, 127.36, 126.78, 125.80, 122.70, 121.10, 120.04, 111.89, 109.42, 83.56, 80.36, 74.23, 58.12, 42.59, 37.93, 30.78, 22.73, 22.65. HRMS (ESI) *m/z* calcd for $C_{24}H_{26}NO_5$ $[M + H]^+$ 408.1811, found 408.1805.

*4.1.4.12. (3aS,5S,9R,9aS,9bS)-9-hydroxy-6,9-dimethyl-3-methylene-2-oxo-2,3,3a,4,5,7,8,9,9a,9b-decahydroazuleno[4,5-b]furan-5-yl 9,10-dioxo-9,10-dihydroanthracene-2-carboxylate (**34**).* White solid; yield 45%. ^{1}H NMR (500 MHz, $CDCl_3$) δ 8.91 (s, 1H, Ar—H), 6.99 (s, 1H, Ar—H), 8.42–8.33 (m, 4H, Ar—H), 7.87–7.83 (m, 1H, Ar—H), 6.26–6.25 (m, 1H, H-13), 5.57 (s, 1H, H-9), 5.52 (s, 1H, H-13), 3.98 (t, J = 10.4 Hz, 1H, H-6), 3.32 (t, J = 11.4 Hz, 1H, H-7), 3.08 (d, J = 10.8 Hz, 1H, H-5), 2.59–2.47 (m, 2H, H-2), 2.33–2.29 (m, 1H, H-8), 2.00–1.78 (m, 6H, H-3, 8, 14), 1.36 (s, 3H, H-15). ^{13}C NMR (126 MHz, $CDCl_3$) δ 182.68, 182.41, 169.31, 164.76, 140.10, 138.19, 136.49, 135.19, 134.84, 134.79, 134.74, 133.83, 133.59, 133.54, 128.97, 128.86, 127.94, 127.72, 127.68, 120.36, 83.70, 80.52, 75.72, 58.46, 42.78, 38.06, 31.10, 31.07, 22.94, 22.92. HRMS (ESI) *m/z* calcd for $C_{30}H_{26}O_7Na$ $[M + Na]^+$ 521.1576, found 521.1570.

*4.1.4.13. (3aS,5S,9R,9aS,9bS)-9-hydroxy-6,9-dimethyl-3-methylene-2-oxo-2,3,3a,4,5,7,8,9,9a,9b-decahydroazuleno[4,5-b]furan-5-yl 3-(2-chloroacetamido)benzoate (**35**).* White solid; yield 59%. ^{1}H NMR (400 MHz, $CDCl_3$) δ 8.33 (s, 1H, NH), 8.06 (t, J = 1.9 Hz, 1H, Ar—H), 7.99–7.67 (m, 2H, Ar—H), 7.46 (t, J = 8.0 Hz, 1H, Ar—H), 6.21 (d, J = 3.4 Hz, 1H, H-13), 5.70 (dd, J = 4.9, 2.0 Hz, 1H, H-9), 5.48 (d, J = 3.4 Hz, 1H, H-13), 4.20 (s, 2H, CO—CH_2), 3.94 (dd, J = 10.8, 10.2 Hz, 1H, H-6), 3.39–3.24 (m, 1H, H-7), 3.13–3.01 (m, 1H, H-5), 2.70 (s, 1H, OH), 2.55–1.38 (m, 9H), 1.35 (s, 3H, H-15). ^{13}C NMR (126 MHz, $CDCl_3$) δ 169.49, 165.43, 164.33, 139.52, 138.35, 137.24, 131.16, 129.69, 129.48, 126.51, 125.18, 121.36, 120.09, 83.71, 80.59, 74.69, 58.22, 43.04, 42.96, 38.24, 30.96, 30.82, 22.92, 22.83. HRMS (ESI) *m/z* calcd for $C_{24}H_{27}NO_6Cl$ $[M + H]^+$ 460.1527, found 460.1521.

*4.1.4.14. (3aS,5S,9R,9aS,9bS)-9-hydroxy-6,9-dimethyl-3-methylene-2-oxo-2,3,3a,4,5,7,8,9,9a,9b-decahydroazuleno[4,5-b]furan-5-yl 2-(5-fluoro-2,4-dioxo-3,4-dihydropyrimidin-1(2H)-yl)acetate (**36**).*. White solid; yield 33%. ^{1}H NMR (400 MHz, $CDCl_3$: CD_3OD = 10:1) δ 7.23 (d, J = 3.0 Hz, 1H, *N*—CH), 6.24 (s, 1H, H-13), 5.52–5.50 (m, 2H, H-9, 13), 4.44 (q, J = 17.0 Hz, 2H), 3.88 (t, J = 10.1 Hz, 1H), 3.21–3.17 (m, 1H, H-7), 2.95–2.89 (m, 1H, H-5), 2.63 (s, 1H, OH), 2.45–2.39 (m, 2H, H-2), 2.24–2.23 (m, 1H, H-8), 1.87–1.68 (m, 6H, H-3, 8, 14), 1.32 (s, 3H, H-15). ^{13}C NMR (126 MHz, $CDCl_3$: CD_3OD = 10:1): δ 169.67, 166.95, 149.72, 141.45, 140.11, 139.56, 137.93, 128.86, 128.59, 128.47, 120.01, 83.19, 80.19, 76.27, 57.79, 42.39, 37.99, 30.64, 30.28, 22.39, 22.30. HRMS (ESI) *m/z* calcd for $C_{21}H_{24}N_2O_7F$ $[M + H]^+$ 435.1568, found 435.1536.

*4.1.4.15. (3aS,5S,9R,9aS,9bS)-9-hydroxy-6,9-dimethyl-3-methylene-2-oxo-2,3,3a,4,5,7,8,9,9a,9b-decahydroazuleno[4,5-b]furan-5-yl 2-(1,3-dioxoisoindolin-2-yl)acetate (**37**).* White solid; yield 39%. ^{1}H NMR (400 MHz, $CDCl_3$) δ 7.91–7.86 (m, 2H, Ar—H), 7.81–7.74 (m, 2H, Ar—H), 6.24–6.22 (m, 1H, H-13), 5.54–5.51 (m, 1H, H-13), 5.50–5.47 (m, 1H, H-9), 4.49–4.43 (m, 2H, CO—CH_2), 3.86–3.80 (m, 1H, H-6), 3.06–3.00 (m, 1H, H-7), 2.72–2.67 (m, 1H, H-5), 2.41–2.33 (m, 2H, H-2), 2.24–2.14 (m, 1H, H-8), 1.78–1.59 (m, 6H, H-3, 8, 14), 1.27 (s, 3H, H-15). ^{13}C NMR (126 MHz, $CDCl_3$) δ 169.33, 167.71, 166.92, 139.83, 137.96, 134.71, 132.04, 128.75, 123.90, 120.38, 83.45, 80.38, 75.70, 58.15, 42.45, 39.46, 37.95, 30.90, 29.91, 22.80, 22.68. HRMS (ESI) *m/z* calcd for $C_{25}H_{26}NO_7$ $[M + H]^+$ 452.1709, found 452.1704.

*4.1.4.16. (3aS,5S,9R,9aS,9bS)-9-hydroxy-6,9-dimethyl-3-methylene-2-oxo-2,3,3a,4,5,7,8,9,9a,9b-decahydroazuleno[4,5-b]furan-5-yl 2-phenoxyacetate (**38**).* White solid; yield 53%. ^{1}H NMR (400 MHz, $CDCl_3$) δ 7.28–7.24 (m, 2H, Ar—H), 6.98–6.94 (m, 1H, Ar—H), 6.88–6.85 (m, 2H, Ar—H), 6.16 (d, J = 3.4 Hz, 1H, H-13), 5.51 (dd, J = 5.0, 2.0 Hz, 1H, H-9), 3.37 (d, J = 3.4 Hz, 1H, H-13), 4.67 (d, J = 1.4 Hz, 2H, CO—CH_2), 3.79 (t, J = 10.4 Hz, 1H, H-6), 2.84–2.77 (m, 1H, H-7), 2.72–2.68 (m, 1H, H-5), 2.33–2.25 (m, 3H, H-2, 8), 1.82–1.74 (m, 5H, H-3, 8, 14), 1.62–1.55 (m, 1H, H-3). ^{13}C NMR (126 MHz, $CDCl_3$) δ 169.32, 168.89, 157.72, 139.98, 138.28, 129.93, 128.67, 122.08, 119.75, 114.42, 83.41, 80.38, 75.07, 65.27, 57.88, 42.24, 38.03, 30.90, 30.55, 22.85, 22.75. HRMS (ESI) *m/z* calcd for $C_{23}H_{26}O_6Na$ $[M + Na]^+$ 421.1621, found 421.1622.

*4.1.4.17. (3aS,5S,9R,9aS,9bS)-9-hydroxy-6,9-dimethyl-3-methylene-2-oxo-2,3,3a,4,5,7,8,9,9a,9b-decahydroazuleno[4,5-b]furan-5-yl 2-((4-fluorophenyl)thio)acetate (**39**).* White solid; yield 68%. ^{1}H NMR (400 MHz, $CDCl_3$) δ 7.40–7.36 (m, 2H, Ar—H), 7.02–6.98 (m, 2H, Ar—H), 6.21 (d, J = 3.4 Hz, 1H, H-13), 5.41–5.38 (m, 2H, H-9, H-13), 3.83 (t, J = 10.7 Hz, 1H, H-6), 3.60 (d, J = 3.5 Hz, 2H, CO—CH_2), 3.01–2.95 (m, 1H, H-7), 2.85–2.81 (m, 1H, H-5), 2.59 (s, 1H, OH), 1.86–1.80 (m, 2H, H-3, 8), 1.71 (s, 1H, H-14), 1.62–1.55 (m, 1H, H-3), 1.30 (s, 3H, H-15). ^{13}C NMR (126 MHz, $CDCl_3$) δ 169.31, 169.30, 163.38 (d, J = 248.2 Hz), 139.65, 138.33, 132.75, 132.68, 129.65 (d, J = 3.7 Hz), 128.88, 119.83, 116.53 (d, J = 22.2 Hz), 116.44, 83.52, 80.41, 75.23, 58.04, 42.37, 38.06, 37.53, 30.92, 30.44, 29.90, 22.86. HRMS (ESI) *m/z* calcd for $C_{23}H_{25}O_5FSNa$ $[M + H]^+$ 433.1479, found 433.1481.

*4.1.4.18. (3aS,5S,9R,9aS,9bS)-9-hydroxy-6,9-dimethyl-3-methylene-2-oxo-2,3,3a,4,5,7,8,9,9a,9b-decahydroazuleno[4,5-b]furan-5-yl 3-(1,3-dioxo-1H-benzo[de]isoquinolin-2(3H)-yl)propanoate (**40**).* White solid;

yield 48%. ^{1}H NMR (400 MHz, $CDCl_3$) δ 8.59 (dd, J = 7.3, 1.1 Hz, 2H, Ar—H), 8.24 (dd, J = 8.3, 1.1 Hz, 2H, Ar—H), 7.79 (dd, J = 8.2, 7.2 Hz, 2H, Ar—H), 6.22 (d, J = 3.4 Hz, 1H, H-13), 3.54 (d, J = 3.4 Hz, 1H, H-13), 5.48–5.46 (m, 1H, H-9), 4.53–4.48 (m, 2H, N—CH_2), 3.85 (dd, J = 11.0, 10.0 Hz, 1H, H-6), 3.19–3.12 (m, 1H, H-7), 2.86–2.78 (m, 3H, H-5, CO—CH_2), 2.48–2.14 (m, 3H, H-2, 8), 1.79–1.75 (m, 5H, H-3, 8, 14), 1.64–1.57 (m, 1H, H-3), 1.28 (s, 3H, H-15). ^{13}C NMR (126 MHz, $CDCl_3$) δ 170.84, 169.51, 163.37, 162.58, 149.95, 139.23, 138.42, 132.83, 130.22, 130.21, 129.87, 129.28, 129.17, 126.78, 124.13, 123.93, 122.85, 120.19, 83.74, 80.42, 74.39, 58.16, 42.62, 38.03, 36.79, 33.10, 30.91, 30.69, 22.87, 22.77. HRMS (ESI) *m/z* calcd for $C_{30}H_{30}NO_7$ $[M + H]^+$ 516.2017, found 516.1997.

*4.1.4.19. (3aS,5S,9R,9aS,9bS)-9-hydroxy-6,9-dimethyl-3-methylene-2-oxo-2,3,3a,4,5,7,8,9,9a,9b-decahydroazuleno[4,5-b]furan-5-yl 4-(4-bromophenyl)-4-oxobutanoate (**41**).* White solid; yield 38%. ^{1}H NMR (400 MHz, $CDCl_3$) δ 7.87–7.76 (m, 2H, Ar—H), 7.68–7.52 (m, 2H, Ar—H), 6.24 (d, J = 3.4 Hz, 1H, H-13), 5.53 (d, J = 3.4 Hz, 1H, H-13), 5.45 (dd, J = 4.7, 2.1 Hz, 1H, H-9), 3.94–3.80 (m, 1H, H-6), 3.36–3.14 (m, 3H, H-7), 2.92–2.82 (m, 1H, H-5), 2.74 (td, J = 6.1, 1.3 Hz, 2H, OCO—CH_2), 2.60 (s, 1H, OH), 2.45–1.58 (m, 9H), 1.30 (s, 3H, H-15). ^{13}C NMR (126 MHz, $CDCl_3$) δ 197.10, 172.50, 169.54, 139.05, 138.36, 135.19, 132.24, 129.67, 129.14, 128.85, 120.18, 83.77, 80.39, 74.35, 58.25, 42.49, 38.04, 33.63, 30.88, 30.74, 28.66, 22.87, 22.74. HRMS (ESI) *m/z* calcd for $C_{25}H_{27}O_6BrNa$ $[M + Na]^+$ 525.0889, found 525.0883.

*4.1.4.20. (3aS,5S,9R,9aS,9bS)-9-hydroxy-6,9-dimethyl-3-methylene-2-oxo-2,3,3a,4,5,7,8,9,9a,9b-decahydroazuleno[4,5-b]furan-5-yl 3-(6,7-dimethoxy-3,4-dihydroisoquinolin-2(1H)-yl)propanoate (**42**).* White solid; yield 42%. ^{1}H NMR (400 MHz, $CDCl_3$) δ 6.54 (s, 1H, Ar—H), 6.47 (s, 1H, Ar—H), 6.03 (d, J = 3.3 Hz, 1H, H-13), 5.41 (dd, J = 4.7, 2.0 Hz, 1H, H-9), 5.28 (d, J = 3.2 Hz, 1H, H-13), 3.82 (d, J = 5.7 Hz, 7H, H-6, OCH_3 × 2), 3.66–3.42 (m, 2H, N—CH_2), 3.11–3.08 (m, 1H, H-5), 2.91–1.38 (m, 19H), 1.27 (s, 3H, H-15). ^{13}C NMR (126 MHz, $CDCl_3$) δ 172.38, 169.30, 147.69, 147.40, 138.93, 138.22, 129.27, 126.24, 125.95, 119.77, 111.51, 109.32, 83.67, 80.39, 74.20, 58.19, 56.06, 55.61, 53.91, 50.97, 42.40, 38.11, 33.38, 30.86, 30.51, 28.88, 22.83, 22.73. HRMS (ESI) *m/z* calcd for $C_{29}H_{38}NO_7$ $[M + H]^+$ 512.2648, found 512.2643.

*4.1.5. General synthesis procedure for compounds **43** and **44***

1.0 mmol of MCL (3), 0.3 mmol of SeO_2 and 0.28 mL of 70% *t*-BuOOH/H_2O were added to 30 mL of dichloromethane. The mixture was stirred and refluxed for 3 h. The resulting mixture was filtered with kieselguhr, and then concentrated under vacuo. The crude residue containing **19**–**22** was mixed with Dess-Martin periodinane (212.0 mg, 0.5 mmol), sodium bicarbonate (840 mg, 10 mmol) and dichloromethane (30 mL). The mixture was stirred for 3 h at room temperature. After the reaction was completed, the solution was quenched with saturated sodium bisulfite solution, and then 30 mL dichloromethane was added. The organic phase was washed with water and brine, dried over anhydrous sodium sulfate, and concentrated in vacuo. The residue was separated by silica gel column chromatography using petroleum ether-ethyl acetate (1:1) to obtain compounds **43** and **44**.

*4.1.5.1. (3aS,9R,9aS,9bS)-9-hydroxy-6,9-dimethyl-3-methylene-3a,7,8,9,9a,9b-hexahydroazuleno[4,5-b]furan-2,5(3H,4H)-dione (**43**).* White solid; yield 49%. ^{1}H NMR (500 MHz, $CDCl_3$) δ 6.34 (d, J = 3.0 Hz, 1H, H-13), 6.62 (d, J = 2.8 Hz, 1H, H-13), 4.30 (t, J = 10.39 Hz, 1H, H-6), 3.16–3.11 (m, 1H, H-7, 8), 3.01 (d, J = 10.4 Hz, 1H, H-5), 2.63–2.52 (m, 2H, H-2, 8), 2.48–2.39 (m, 1H, H-2), 2.00–1.90 (m, 2H, H-3), 1.83 (s, 3H, H-15), 1.33 (s, 3H, H-14). ^{13}C NMR (100 MHz, $CDCl_3$) δ 197.33, 168.62, 150.19, 136.88, 133.84, 121.72, 81.97, 79.88, 60.77, 42.82, 42.29, 37.02, 31.62, 22.45, 16.94. HRMS (ESI) *m/z* calcd for $C_{15}H_{19}O_4$ $[M + H]^+$ 263.1283, found 263.1265.

*4.1.5.2. (3aS,9R,9aS,9bS)-9-hydroxy-6,9,9a-trimethyl-3-methylene-3,3a,4,5,8,9,9a,9b-octahydroazuleno[4,5-b]furan-2,7-dione (**44**).* White solid; yield 13%. ^{1}H NMR (400 MHz, $CDCl_3$) δ 6.27 (d, J = 3.3 Hz, 1H, H-13), 5.56 (d, J = 3.3 Hz, 1H, H-13), 3.88 (t, J = 10.2 Hz, 1H, H-6), 3.22–3.18 (m, 1H, H-5), 2.81–2.73 (m, 2H, H-3,7), 2.67 (s, 1H, OH), 2.53–2.45 (m, 3H, H-3, 9), 2.36 (d, J = 2.7 Hz), 2.23–2.16 (m, 1H, H-8), 1.50–1.47 (m, 1H, H-8), 1.38 (s, 3H, H-15). ^{13}C NMR (100 MHz, $CDCl_3$) δ 201.66, 169.06, 155.48, 137.92, 130.67, 120.23, 83.12, 73.89, 58.34, 54.58, 49.57, 38.75, 24.85, 24.44, 24.11. HRMS (ESI) *m/z* calcd for $C_{15}H_{19}O_4$ $[M + H]^+$ 263.1283, found 263.1264.

4.2. Materials for biological studies

4.2.1. Cell culture

Human glioblastoma cell lines U87MG, hepatocellular carcinoma cell lines HepG2, Human colorectal carcinomas cell lines HCT116 and gastric carcinoma cell lines BGC823 were purchased from Peking Union Medical College (Beijing, China). Human lung adenocarcinoma cell lines PC-9 was purchased from Shanghai Xiangf Bio Company.

U87MG cell was cultured in MEM Minimum Essential Medium (MEM; Gibco, Inc., Gaithersburg, MD, USA), other cells were cultured in DMEM Dulbecco's Modified Eagle Medium (DMEM; Gibco Inc., Gaithersburg, MD, USA). All cultures were provided with 10% fetal bovine serum (FBS; YHSM, Beijing, China), 100 IU/mL penicillin, and 100 μg/mL streptomycin, and cells were incubated at 37C in an atmosphere of 5% CO_2.

4.2.2. Cell proliferation assay

Cells were added 100 μL to each well of a 96-well plate and cultured for 24 h. 1.5 × 10^4 cells were seeded in each well. The cells were treated with different concentrations of synthesized compounds for 120 h. MTT reagent (50 μL, 2.0 mg/mL, Beijing Solarbio Science & Technology Co., Ltd, Beijing, China) was added to each well and cultured for a further 2 h. The solution was removed and 200 μL DMSO (Biosharp, Inc., Hefei, China) was added. The optical density at 570 nm was measured using an ELISA reader (WD-2102A; Beijing Liuyi Biology Co., Ltd, Beijing, China). The median inhibitory concentration (IC_{50}) was determined from the dose–response curve. Experiments were performed in triplicate.

4.2.3. Animal assay

All animal experiments were performed and approved by the Animal Care and Use Committee of Chinese Academy of Medical Sciences and Peking Union Medical College.

4.2.3.1. In vivo pharmacokinetics study. Before the experiment, compound **31** were dissolved with PEG400, then diluted with double distilled water, and ultrasonically made into suspension (PEG400 was 25 vol%). The concentration of suspension was 10 mg/ml. Male Kunming mice, weighing 22–24 g, were obtained from Beijing Vital River Experimental Animal Co., Ltd (License number: SCXK 2016-0011). Three male mice were orally given compound **31** (100 mg/kg), the blood was collected in 1.5 mL heparinized polythene tubes containing NaF by orbital bleeding via capillary tubes at 0 min, 5 min, 10 min, 15 min, 30 min, 1 h, 2 h, 4 h, 6 h, 8 h, 12 h and 24 h. The blood was placed on ice, then centrifuged at 8000 rpm for 5 min. The plasma was separated and frozen at −20 °C until analysis. Chromatographic separations were carried out on Zorbax C18 column (3.5 μm, 2.1 mm × 100 mm). The column temperature was set to 30 °C. The mobile phase consisted of methanol (0.1% formic acid) and deionized water (0.1% formic acid) with gradient elution at a flow rate of 0.2 mL/min.

4.2.3.2. H22 hepatocellular carcinoma model. Kunming mice (male, 15.0–17.0 g) for research of PTL esters and MCL esters were purchased from Beijing Hfk Bioscience Co., Ltd (Beijing, China) and Kunming mice

(male, 16.0–18.0 g) for compound **43** were purchased from National Institutes for Food and Drug Control. Under sterile conditions, H22 tumor tissue was diluted to cell suspension by normal saline in a ratio of 1:3, mice were subcutaneously implanted with 0.2 mL of the H22 tissue cell suspension in their left flank. After inoculation for 24 h, the tumor-bearing mice were divided into six groups with seven animals in each group in research of PTL esters and six groups with six animals in each group in research of MCL esters and five groups with eight animals in research of effects of compound **43** doses in G422-bearing mice (seven animals in group 10.0 mg/kg). Drugs were administered as follows in H22 murine model of PTL esters: Group 1: 25% PEG (control), Group 2: 40.0 mg/kg 5-FU, Group 3: 30.0 mg/kg of 16, Group 4: 60.0 mg/kg of 16, Group 5: 40.0 mg/kg of 18, Group 6: 80.0 mg/kg of 18. PEG400 and 16 and 18 were orally administrated for 5 days and 5-FU was once every three days by intraperitoneal injection. Drugs were administered as follows in H22 murine model of MCL esters: Group 1: 25% PEG (control), Group 2: 60.0 mg/kg CTX, Group 3: 100.0 mg/kg of **25**, Group 4: 10.0 mg/kg of **30**, Group 5: 10.0 mg/kg of **31**, Group 6: 10.0 mg/kg of **43**. PEG400 and MCL esters were orally administrated for 9 days and CTX was once a week by intraperitoneal injection. Drugs were administered as follows in H22 murine model for compound **43**: Group 1: 25% PEG (control), Group 2: 40.0 mg/kg 5-FU, Group 3: 10.0 mg/kg of compound **43**, Group 4: 20.0 mg/kg of compound **43**, Group 5: 30.0 mg/kg of compound **43**. PEG400 and compound **43** were orally administrated for 7 days, and 5-FU was once every three days by intraperitoneal injection. Mice were euthanized and their tumors were excised, weighed, and photographed. Tumors were weighed and photographed, and the inhibition rate was measured. Tumors were stored at −80 °C until further analysis.

4.2.3.3. C26 colon carcinoma model. BALB/C mice (male, 16.0 g) were purchased from Beijing Hfk Bioscience Co., Ltd (Beijing, China). C26 tumor tissue was diluted to cell suspension by normal saline in a ratio of 1:10 under sterile conditions, and cell suspension were subcutaneously implanted with 0.2 mL in the left flank of each mouse. After inoculation for 24 h, tumor-bearing mice were randomly separated into six groups with 6 animals in each group. One group received p.o. of 25% PEG400 for 12 days as a model control group, another group received an intraperitoneal injection of 40.0 mg/kg 5-FU (once every three days), and the remaining 4 groups received p.o. of 30.0 mg/kg and 60.0 mg/kg for compound **16**, and 40.0 mg/kg and 80.0 mg/kg for compound **18** respectively for 12 days. Tumors were weighed and photographed, and the inhibition rate was measured. Tumors were stored at − 80 °C until further analysis.

4.2.3.4. G422 glioblastoma model. Kunming mice (male, 16.0–18.0 g) in research of MCL derivatives and compound **43** were purchased from Beijing Hfk Bioscience Co., Ltd (Beijing, China). G422 tumor tissue was diluted to cell suspension by normal saline in a ratio of 1:3, mice were subcutaneously implanted with 0.2 mL of the G422 tissue cell suspension in their left flank. After inoculation for 24 h, the tumor-bearing mice were divided into five groups with five animals in each group in research of MCL derivatives and six groups with seven animals in research of effect of compound **43** in G422 glioblastoma model. Drugs were administered as follows in research of MCL derivatives: Group 1: 25% PEG (control), Group 2: 30.0 mg/kg TMZ, Group 3: 100.0 mg/kg of compound **30**, Group 4: 100.0 mg/kg of compound **31**, Group 5: 100.0 mg/kg of compound **43**. PEG400 and compounds **30**, **31** and **43** were orally administrated for 13 days, and TMZ was administered an oral dose of 30.0 mg/kg for 5 days. Drugs were administered as follows in G422-bearing mice for compound **43**: Group 1: 25% PEG (control), Group 2: 30.0 mg/kg TMZ, Group 3: 10.0 mg/kg of compound **43**, Group 4: 20.0 mg/kg of compound **43**, Group 5: 40.0 mg/kg of compound **43**, Group 6: 60.0 mg/kg of compound **43**. PEG400 and compound **43** were orally administrated for 12 days, and TMZ was administered an oral dose of 30.0 mg/kg for 5 days. Mice were euthanized and their tumors were excised, weighed, and photographed. Tumors were weighed and photographed, and the inhibition rate was measured. Tumors were stored at − 80 °C until further analysis.

4.2.4. Luciferase reporter assay

The NF-κB luciferase reporter plasmid and STAT3 luciferase reporter plasmids were obtained from Ningbo Eastinno Biotechnology, China. HepG2 cells were seeded onto 96-well plates at a density of 2.5×10^4 cells per well for 24 h. Cells were then transfected with firefly-luciferase reporter plasmid for 48 h. After the transfection, the cells were treated simultaneously with the corresponding activator and different concentrations of tested compounds. The activator was 50 ng/mL of TNF-α (Peprotech) for NF-κB-reporter assay or 10 ng/mL of IL-6 (Peprotech) for STAT3. After 5 h of treatment for NF-κB assay or 24 h of treatment for STAT3 assay, the cells were harvested and the luciferase activity was measured using Promega ONE-Glo Luciferase Assay System following the standard protocol.

4.2.5. Cell apoptosis study

The effect of compound on cell apoptosis was studied using AnnexinV-FITC/PI labeled Apoptosis Assay Kit (BestBio, Shanghai, China) following the manufacturer's instructions. In brief, cells were cultured into 6-well plates and incubated for 48 h. Then, cells with exponential growth were treated with 0 μM, 1 μM, 2 μM, 4 μM, 8 μM and 16 μM of compound **43** in DMSO for 12 h. After the cells were collected and washed twice with cold phosphate buffer solution and once with binding buffer, cells were stained by 5 μL of AnnexinV-FITC and 5 μL of PI. Apoptotic cells were analyzed by a flow cytometry ACEA Novocyte.

Ethical approval

All procedures performed in studies involving animals are in compliance with the ethical standards of the Animal Care and Use Committee of Chinese Academy of Medical Science and Peking Union Medical College, China (00005909, 00005910, 00003128) and in accordance with the National Laboratory Animal Management Regulations (Directive 2017/10/China).

Declaration of Competing Interest

The authors declare that they have no known competing financial interests or personal relationships that could have appeared to influence the work reported in this paper.

Acknowledgements

This work was supported by the National Drug Innovation Major Project (2018ZX09711-001-005, 2018ZX09721003-008-026) and Chinese Academy of Medical Sciences (CAMS) Initiation fund for Medical Science (2016-I2M-1-008).

Appendix A. Supplementary material

Supplementary data to this article can be found online at https://doi.org/10.1016/j.bioorg.2021.104973.

References

[1] A. Ghantous, A. Sinjab, Z. Herceg, N. Darwiche, Parthenolide: from plant shoots to cancer roots, Drug Discov. Today 18 (2013) 894–905.
[2] R.R.A. Freund, P. Gobrecht, D. Fischer, H.-D. Arndt, Advances in chemistry and bioactivity of parthenolide, Nat. Prod. Rep. 37 (2020) 541–565.
[3] M.R.O. Kreuger, S. Grootjans, M.W. Biavatti, P. Vandenabeele, K. D'Herde, Sesquiterpene lactones as drugs with multiple targets in cancer treatment: focus on parthenolide, Anticancer Drugs 23 (2012) 883–896.
[4] M. Sztiller-Sikorska, M. Czyz, Parthenolide as cooperating agent for anti-cancer treatment of various malignancies, Pharmaceuticals 13 (2020) 194.

[5] V.B. Mathema, Y.-S. Koh, B.C. Thakuri, M. Sillanpää, Parthenolide, a Sesquiterpene Lactone, Expresses Multiple Anti-cancer and Anti-inflammatory Activities, Inflammation 35 (2012) 560–565.
[6] J.-D. Zhai, D. Li, J. Long, H.-L. Zhang, J.-P. Lin, C.-J. Qiu, Q. Zhang, Y. Chen, Biomimetic Semisynthesis of Arglabin from Parthenolide, J. Org. Chem. 77 (2012) 7103–7107.
[7] E. Viennois, B. Xiao, S. Ayyadurai, L. Wang, P.G. Wang, Q. Zhang, Y. Chen, D. Merlin, Micheliolide, a new sesquiterpene lactone that inhibits intestinal inflammation and colitis-associated cancer, Lab. Invest. 94 (2014) 950–965.
[8] J. Zhong, W. Gong, J. Chen, Y. Qing, S. Wu, H. Li, C. Huang, Y. Chen, Y. Wang, Z. Xu, W. Liu, H. Li, H. Long, Micheliolide alleviates hepatic steatosis in db/db mice by inhibiting inflammation and promoting autophagy via PPAR-γ-mediated NF-κB and AMPK/mTOR signaling, Int. Immunopharmacol. 59 (2018) 197–208.
[9] X. Tang, Q. Ding, C. Chen, F. Chen, X. Zhou, C.J. Hong, W. Pan, Micheliolide inhibits gastric cancer growth in vitro and in vivo via blockade of the IL-6/STAT3 pathway, Pharmazie 74 (2019) 175–178.
[10] J. Li, S. Li, J. Guo, Q. Li, J. Long, C. Ma, Y. Ding, C. Yan, L. Li, Z. Wu, H. Zhu, K. K. Li, L. Wen, Q. Zhang, Q. Xue, C. Zhao, N. Liu, I. Ivanov, M. Luo, R. Xi, H. Long, P. G. Wang, Y. Chen, Natural Product Micheliolide (MCL) Irreversibly Activates Pyruvate Kinase M2 and Suppresses Leukemia, J. Med. Chem. 61 (2018) 4155–4164.
[11] X. Qin, X. Jiang, X. Jiang, Y. Wang, Z. Miao, W. He, G. Yang, Z. Lv, Y. Yu, Y. Zheng, Micheliolide inhibits LPS-induced inflammatory response and protects mice from LPS challenge, Sci. Rep.-Uk 6 (2016) 23240.
[12] Q. Li, Y. Sun, B. Liu, J. Li, X. Hao, W. Ge, X. Zhang, S. Bao, J. Gong, Z. Jiang, C. Qiu, L. Zhao, Y. Zhao, Y. Chen, X. Yang, Y. Ding, Z. Wu, ACT001 modulates the NF-κB/MnSOD/ROS axis by targeting IKKβ to inhibit glioblastoma cell growth, J. Mol. Med. 98 (2020) 263–277.
[13] D.R. Johnson, B.P. O'Neill, Glioblastoma survival in the United States before and during the temozolomide era, J. Neurooncol. 107 (2012) 359–364.
[14] W.W. Ma, Q.Q. Shi, Y.H. Ding, J. Long, Q. Zhang, Y. Chen, Synthesis of Micheliolide Derivatives and Their Activities against AML Progenitor Cells, Molecules 18 (2013) 5980–5992.
[15] R. Fasan, S. Giovani, H. Alwaseem, Micheliolide derivatives, methods for their preparation and their use as anticancer and antiinflammatory agents, WO 2019/040335 A1, August 17, 2018.
[16] Q. Zhang, Y. Lu, Y. Ding, J. Zhai, Q. Ji, W. Ma, M. Yang, H. Fan, J. Long, Z. Tong, Y. Shi, Y. Jia, B. Han, W. Zhang, C. Qiu, X. Ma, Q. Li, Q. Shi, H. Zhang, D. Li, J. Zhang, J. Lin, L.-Y. Li, Y. Gao, Y. Chen, Guaianolide Sesquiterpene Lactones, a Source To Discover Agents That Selectively Inhibit Acute Myelogenous Leukemia Stem and Progenitor Cells, J. Med. Chem. 55 (2012) 8757–8769.
[17] Y.-H. Ding, H.-X. Fan, J. Long, Q. Zhang, Y. Chen, The application of Heck reaction in the synthesis of guaianolide sesquiterpene lactones derivatives selectively inhibiting resistant acute leukemic cells, Bioorg. Med. Chem. Lett. 23 (2013) 6087–6092.
[18] S. Bommagani, J. Ponder, N.R. Penthala, V. Janganati, C.T. Jordan, M.J. Borrelli, P. A. Crooks, Indole carboxylic acid esters of melampomagnolide B are potent anticancer agents against both hematological and solid tumor cells, Eur. J. Med. Chem. 136 (2017) 393–405.
[19] Y. Ding, S. Li, W. Ge, Z. Liu, X. Zhang, M. Wang, T. Chen, Y. Chen, Q. Zhang, Design and synthesis of parthenolide and 5-fluorouracil conjugates as potential anticancer agents against drug resistant hepatocellular carcinoma, Eur. J. Med. Chem. 183 (2019), 111706.
[20] W. Ge, X. Hao, F. Han, Z. Liu, T. Wang, M. Wang, N. Chen, Y. Ding, Y. Chen, Q. Zhang, Synthesis and structure-activity relationship studies of parthenolide derivatives as potential anti-triple negative breast cancer agents, Eur. J. Med. Chem. 166 (2019) 445–469.
[21] D.-Z. Li, Q.-Z. Zhang, C.-Y. Wang, Y.-L. Zhang, X.-Y. Li, J.-T. Huang, H.-Y. Liu, Z.-D. Fu, H.-X. Song, J.-P. Lin, T.-F. Ji, X.-D. Pan, Synthesis and antitumor activity of novel substituted uracil-1′(N)-acetic acid ester derivatives of 20(S)-camptothecins, Eur. J. Med. Chem. 125 (2017) 1235–1246.
[22] N.M. Patel, S. Nozaki, N.H. Shortle, P. Bhat-Nakshatri, T.R. Newton, S. Rice, V. Gelfanov, S.H. Boswell, R.J. Goulet, G.W. Sledge, H. Nakshatri, Paclitaxel sensitivity of breast cancer cells with constitutively active NF-κB is enhanced by IκBα super-repressor and parthenolide, Oncogene 19 (2000) 4159–4169.
[23] A. D'Anneo, D. Carlisi, M. Lauricella, R. Puleio, R. Martinez, S. Di Bella, P. Di Marco, S. Emanuele, R. Di Fiore, A. Guercio, R. Vento, G. Tesoriere, Parthenolide generates reactive oxygen species and autophagy in MDA-MB231 cells. A soluble parthenolide analogue inhibits tumour growth and metastasis in a xenograft model of breast cancer, Cell Death Dis. 4 (2013) e891–e891.
[24] S. Nasim, S. Pei, F.K. Hagen, C.T. Jordan, P.A. Crooks, Melampomagnolide B: A new antileukemic sesquiterpene, Bioorg. Med. Chem. 19 (2011) 1515–1519.
[25] Z.-J. Yang, W.-Z. Ge, Q.-Y. Li, Y. Lu, J.-M. Gong, B.-J. Kuang, X. Xi, H. Wu, Q. Zhang, Y. Chen, Syntheses and Biological Evaluation of Costunolide, Parthenolide, and Their Fluorinated Analogues, J. Med. Chem. 58 (2015) 7007–7020.
[26] N.H. Zuma, J. Aucamp, D.D. N'Da, An update on derivatisation and repurposing of clinical nitrofuran drugs, Eur. J. Pharm. Sci. 140 (2019), 105092.
[27] X. Jia, Q. Liu, S. Wang, B. Zeng, G. Du, C. Zhang, Y. Li, Synthesis, cytotoxicity, and in vivo antitumor activity study of parthenolide semicarbazones and thiosemicarbazones, Bioorg. Med. Chem. 28 (2020), 115557.
[28] M.S. Mitchell, R.C. Deconti, Immunosuppression by 5-fluorouracil, Cancer 26 (1970) 884–889.
[29] T.S. Armstrong, Y. Cao, M.E. Scheurer, E. Vera-Bolaños, R. Manning, M.F. Okcu, M. Bondy, R. Zhou, M.R. Gilbert, Risk analysis of severe myelotoxicity with temozolomide: The effects of clinical and genetic factors, Neuro-Oncology 11 (2009) 825–832.
[30] J. Sahler, J.J. Bernard, S.L. Spinelli, N. Blumberg, R.P. Phipps, The Feverfew plant-derived compound, parthenolide enhances platelet production and attenuates platelet activation through NF-κB inhibition, Thromb. Res. 127 (2011) 426–434.
[31] D.E. Johnson, R.A. O'Keefe, J.R. Grandis, Targeting the IL-6/JAK/STAT3 signalling axis in cancer, Nat. Rev. Clin. Oncol. 15 (2018) 234–248.
[32] N.D. Perkins, Integrating cell-signalling pathways with NF-κB and IKK function, Nat. Rev. Mol. Cell Biol. 8 (2007) 49–62.
[33] V. Baud, M. Karin, Is NF-κB a good target for cancer therapy? Hopes and pitfalls, Nat. Rev. Drug Discov. 8 (2009) 33–40.
[34] G. He, M. Karin, NF-κB and STAT3 – key players in liver inflammation and cancer, Cell Res. 21 (2011) 159–168.
[35] D. Carlisi, A. D'Anneo, L. Angileri, M. Lauricella, S. Emanuele, A. Santulli, R. Vento, G. Tesoriere, Parthenolide sensitizes hepatocellular carcinoma cells to trail by inducing the expression of death receptors through inhibition of STAT3 activation, J. Cell. Physiol. 226 (2011) 1632–1641.
[36] Y. Ding, Q. Xue, S. Liu, K. Hu, D. Wang, T. Wang, Y. Li, H. Guo, X. Hao, W. Ge, Y. Zhang, A. Li, J. Li, Y. Chen, Q. Zhang, Identification of Parthenolide Dimers as Activators of Pyruvate Kinase M2 in Xenografts of Glioblastoma Multiforme in Vivo, J. Med. Chem. 63 (2020) 1597–1611.
[37] E.H. Krenske, R.C. Petter, Z. Zhu, K.N. Houk, Transition States and Energetics of Nucleophilic Additions of Thiols to Substituted α,β-Unsaturated Ketones: Substituent Effects Involve Enone Stabilization, Product Branching, and Solvation, J. Org. Chem. 76 (2011) 5074–5081.
[38] S. Amslinger, The Tunable Functionality of α,β-Unsaturated Carbonyl Compounds Enables Their Differential Application in Biological Systems, ChemMedChem 5 (2010) 351–356.
[39] A.J. García-Piñeres, V.C. Castro, G. Mora, T.J. Schmidt, E. Strunck, H.L. Pahl, I. Merfort, Cysteine 38 in p65/NF-κB Plays a Crucial Role in DNA Binding Inhibition by Sesquiterpene Lactones, J Biol Chem, 276 (2001) 39713-39720.
[40] Y.-I. Hahn, S.-J. Kim, B.-Y. Choi, K.-C. Cho, R. Bandu, K.P. Kim, D.-H. Kim, W. Kim, J.S. Park, B.W. Han, J. Lee, H.-K. Na, Y.-N. Cha, Y.-J. Surh, Curcumin interacts directly with the Cysteine 259 residue of STAT3 and induces apoptosis in H-Ras transformed human mammary epithelial cells, Sci. Rep.-Uk 8 (2018) 6409.
[41] N. Don-Doncow, Z. Escobar, M. Johansson, S. Kjellström, V. Garcia, E. Munoz, O. Sterner, A. Bjartell, R. Hellsten, Galiellalactone Is a Direct Inhibitor of the Transcription Factor STAT3 in Prostate Cancer Cells, J. Biol. Chem. 289 (2014) 15969–15978.
[42] S.A. Holstein, R.J. Hohl, Synergistic Interaction of Lovastatin and Paclitaxel in Human Cancer Cells, Mol. Cancer Ther. 1 (2001) 141–149.
[43] J.F. de Oliveira, A.L. da Silva, D.B. Vendramini-Costa, C.A.D. Amorim, J. F. Campos, A.G. Ribeiro, R.O. de Moura, J.L. Neves, A.L.T.G. Ruiz, J.E. de Carvalho, M.D.A. de Lima, Synthesis of thiophene-thiosemicarbazone derivatives and evaluation of their in vitro and in vivo antitumor activities, Eur. J. Med. Chem. 104 (2015) 148–156.
[44] Y.J. Kang, Z.-X. Zhou, G.-W. Wang, A. Buridi, J.B. Klein, Suppression by Metallothionein of Doxorubicin-induced Cardiomyocyte Apoptosis through Inhibition of p38 Mitogen-activated Protein Kinases, J. Biol. Chem. 275 (2000) 13690–13698.